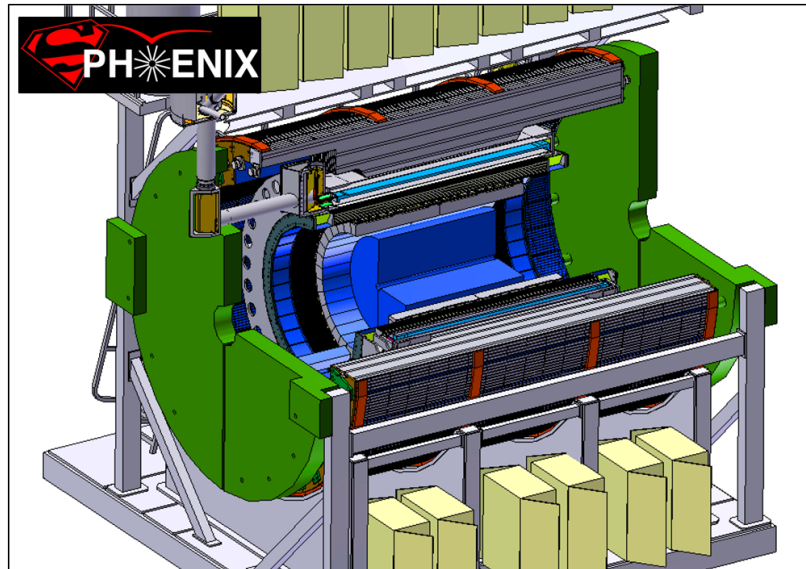
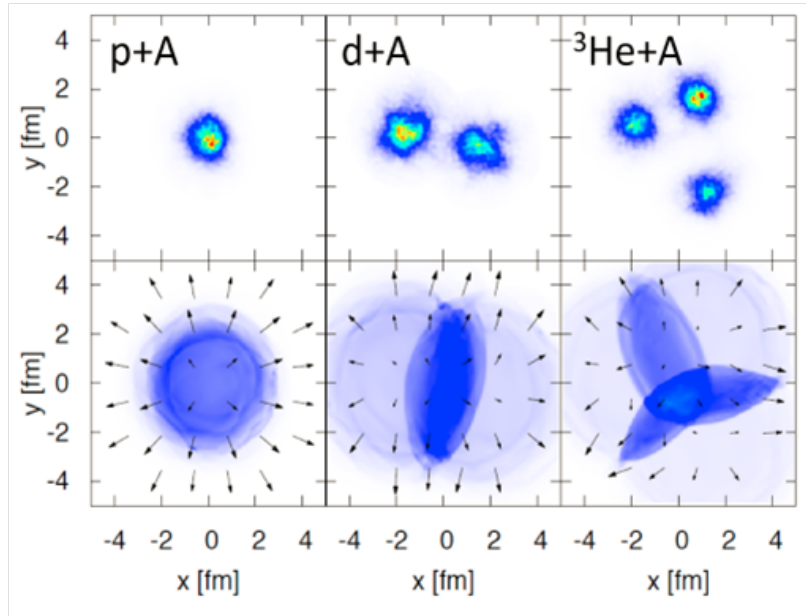


PHENIX Beam Use Proposal Run-16 and Run-17

Submitted May 18, 2015



Executive Summary

The PHENIX Collaboration is at a very exciting point in time with excellent high-statistics data sets in $p+p$ at 510 GeV from Run-13 and Au+Au at 200 GeV from Run-14, combined with new collision systems of $^3\text{He}+\text{Au}$ at 200 GeV from Run-14 and nearing completion of Run-15 with polarized $p+p$ and polarized $p+A$ at 200 GeV. At this same point, the sPHENIX proposal has recently completed a positive Department of Energy Science review and is moving rapidly forward towards a Cost and Schedule Review. The PHENIX experiment will take data in Run-16, and then the detector will be decommissioned to make way for full installation of sPHENIX with first physics data taking projected for 2021.

In this document we propose a physics program for Run-16 that is driven by exciting recent developments in theory and experimental data publications. In 2014, the NPP Program Advisory Committee recommended ten weeks of physics running with Au+Au at 200 GeV as its “highest priority” and we have incorporated this into our proposal. We discuss in the proposal the different options strongly considered by the collaboration for the remaining cryo-weeks available and prioritize between them. In fact, we believe a Run-16 run plan consisting solely of Option A (Section 3.3) and Option B (Section 3.4) delivers a compelling physics program and would be a more effective exploitation of the physics capabilities of the PHENIX detector in its final data taking run. We understand that a broad optimization of priorities will need to be done considering both PHENIX and STAR requests, EIC R&D requirements, and the fact that PHENIX will only be participating in Run-16.

The official beam use proposal charge (included as Appendix A) requested a plan for 22 cryo-weeks in Run-16 and for 15 or 22 cryo-weeks in Run-17. We do not include a proposal for Run-17 since at that time the PHENIX detector will be decommissioned.

The PHENIX collaboration request is as follows.

Run-16 Proposal (22 cryo-weeks)

Au+Au @ 200 GeV for 10 weeks

Physics driven goal is 1.8 nb^{-1} (12 billion minimum bias events) recorded within $|z| < 10 \text{ cm}$

Option A: Au+Au and $p+p$ @ 62.4 GeV Program

Au+Au @ 62.4 GeV for 5 weeks

Physics driven goal is 0.22 nb^{-1} (1.5 billion minimum bias events) recorded within $|z| < 10 \text{ cm}$

$p+p$ @ 62.4 GeV for 2 weeks, $\langle \mathcal{P} \rangle = 60\%$

Physics driven goal is 0.25 pb^{-1} (10 billion trigger sampled events) recorded within $|z| < 10 \text{ cm}$

Option B: d +Au Beam Energy Scan

200 GeV for 1.5 weeks, 62.4 GeV for 1.5 weeks, 39 GeV for 2 weeks, 20 GeV for 2 weeks

Physics driven goal is 2400, 230, 110, 7 million central events for the four energies respectively recorded within $|z| < 10 \text{ cm}$

As noted above, we include in our Beam Use Proposal the ten weeks of Au+Au at 200 GeV data taking — as detailed in Section 3.2. We project recording 1.8 nb^{-1} , compared to the 2.3 nb^{-1} recorded in the longer and very successful Run-14 (which was 40% above our initial goal for that run).

As detailed in the PHENIX Beam Use Proposal submitted in 2014 [1], we proposed an extensive program of investigating heavy flavor production and in-medium modification through a high-statistics data taking of $p+p$, $p(d)+\text{Au}$, and Au+Au at a collision energy of 62.4 GeV. As detailed in this proposal, see Section 3.3, this physics has become even more compelling with recent theoretical expectations of the influence of stronger heavy quark to medium coupling near the transition temperature and with the publication of PHENIX heavy flavor electron results from data taken in 2010 [2], prior to the installation of precision silicon vertex trackers. We also highlight the intriguing potential for a measurement of a longitudinal-transverse asymmetry, A_{LT} , in cross-polarized $p+p$ at 62.4 GeV, further exploiting the unique capabilities of RHIC. Given the constraint of including ten physics weeks of running for Au+Au at 200 GeV within the Run-16 plan, the 62.4 GeV program is rather constrained. At the same time, detailed projections indicate a very interesting program with sufficient running of $p+p$ and Au+Au at 62.4 GeV that will provide crucial constraints on models of heavy quark interactions in the quark-gluon plasma.

The Collaboration has also investigated running a small-system beam energy scan. Guidance from C-AD indicates that only d +Au collisions (as opposed to p +Au or ^3He +Au) would be available in Run-16 due to constraints imposed by the Electron Ion Collider (EIC) R&D test for Coherent electron Cooling (CeC). In the running time available, an excellent d +Au program at four collision energies (20, 39, 62.4, and 200 GeV) would provide very interesting constraints on “flow-like” patterns already observed in high multiplicity $p+p$ and $p+\text{Pb}$ events at the LHC and d +Au and

$^3\text{He}+\text{Au}$ at RHIC. This option is detailed in Section 3.4 and indicates a highly impactful physics program uniquely enabled at RHIC.

The Collaboration has a continued, strong interest in the polarized $p+p$ program at 510 GeV, both in longitudinal and transverse spin physics. We detail these interests in Section 3.5. However, in the running time available in 2016, we do not find this program is sufficiently impactful to be our highest priority.

In this document, we first present highlights of recent scientific accomplishments by the PHENIX Collaboration. This is followed by updates on the FVTX, VTX and MPC-EX upgrades. We then present the details and priorities of the PHENIX Beam Use Proposal. Lastly, we present recent developments regarding our plans for sPHENIX. We highlight that sPHENIX has recently passed the Department of Energy Science Review for the project.

Contents

1 Recent scientific accomplishments	1
1.1 Small-System Results	1
1.2 Beam Energy Scan	2
1.3 Characterizing the QGP	4
1.4 Spin Physics	7
1.5 Beyond the Standard Model	8
2 Status of upgrades	11
2.1 Forward silicon vertex detector (FVTX)	11
2.2 Barrel silicon vertex detector (VTX)	15
2.3 Muon piston calorimeter extension (MPC-EX)	18
3 Proposal for Run-16	21
3.1 Accelerator performance and luminosity estimates	21
3.2 Run-16 Au+Au at 200 GeV Running	22
3.3 Run-16 Au+Au and $p+p$ 62 GeV Program	24
3.3.1 Spin physics at 62.4 GeV	28
3.4 Run-16 Small-System ($d+A$) Beam Energy Scan	31
3.5 Options for $p+p$ at 510 GeV Running	35
4 sPHENIX	39
A Beam use proposal charge	43
References	45

Chapter 1

Recent scientific accomplishments

The PHENIX Collaboration continues to be extremely productive, with fifteen peer-reviewed publications in the year since the last PAC meeting. Here we briefly highlight some of the many scientific accomplishments of the last year, and also indicate the results we are working toward finalizing in the near future.

1.1 Small-System Results

The Collaboration has continued its investigations of possible quark-gluon plasma formation in small systems, in particular $d+Au$, ^3He+Au . Now in Run-15 we are extending this to include $p+Au$, $p+Al$ and high multiplicity $p+p$. In our last beam use proposal, we highlighted our results on elliptic flow coefficient v_2 as a function of p_T in $d+Au$, with and without particle identification. These results will soon be published in Physical Review Letters and will be highlighted as a “PRL Editors’ Suggestion” [3].

The wide interest in the physics of small systems led PHENIX to a push for a ^3He+Au run, exploiting the unique capabilities of RHIC. The success of the Run-14 Au+Au data taking (exceeding our integrated luminosity goals by 40%), enabled a short ^3He+Au run at the end of Run-14. The ^3He+Au run was very successful and PHENIX collected 2.2 billion events. PHENIX used, for the first time, a centrality trigger based on multiplicity in the beam-beam counters (BBC) to enhance the 0-5% most central event sample by nearly an order of magnitude. The forward silicon vertex detectors (FVTX) were used to determine the reaction plane for these measurements, providing a substantially improved reaction plane resolution.

Preliminary results from the ^3He+Au data set were shown at the Initial Stages 2014 Conference in December 2014. Figure 1.1 shows a comparison of those results with a number of current theory calculations. The results have been finalized and a paper will soon be submitted to the journals. Notably, the agreement between SONIC, a viscous hydrodynamic model, and the data is improved by the addition of pre-hydrodynamic flow, as implemented in the SUPERSONIC model [4]. Hydrodynamics translates initial anisotropies in geometry into momentum anisotropies. However, small systems such as ^3He+Au may not live long enough prior to hadronic freeze out for the flow that develops as a result of hydrodynamic evolution to overwhelm pre-equilibrium

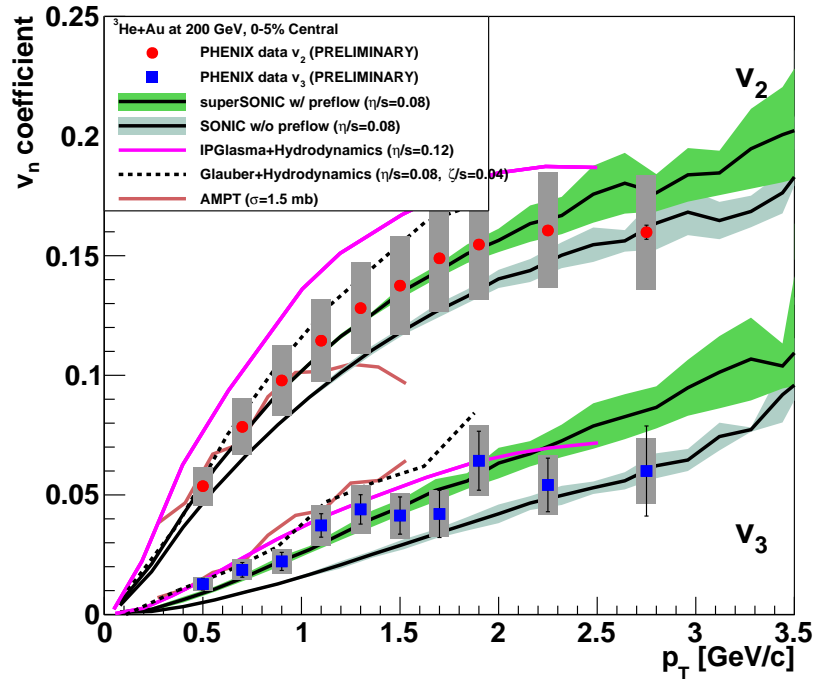


Figure 1.1: PHENIX Preliminary measurements of v_2 and v_3 in 0-5% central $^3\text{He}+\text{Au}$ compared to several theory calculations.

sources of azimuthal flow. Systems such as $^3\text{He}+\text{Au}$, $d+\text{Au}$, and $p+\text{Au}$, seem to alter the relative importance of mechanisms contributing to the momentum anisotropies observed in the final state, enabling the disentanglement of those contributions and insight into the physics. We have a host of analyses of the $^3\text{He}+\text{Au}$ data set in progress including flow coefficients to much higher p_T , with particle identification, and additional correlation observables.

In Run-15, we successfully implemented a $p+p$ high multiplicity trigger to look for such effects in the smallest systems — as observed by CMS at the LHC [5]. Details on the FVTX based trigger are given in Section 2.1. We are in the middle of data taking in $p+\text{Au}$ collisions, and we look forward to a short run of $p+\text{Al}$ at the end of Run-15.

These results in small systems strongly motivate our run proposal for a Small-System Beam Energy Scan detailed in Section 3.4.

1.2 Beam Energy Scan

The PHENIX Collaboration has successfully taken data in Au+Au collisions over a broad range of energies (7.7–200 GeV). We have submitted for publication a paper presenting a complete set of HBT results over the energy range 39–200 GeV [6]. As shown in Figure 1.2, the Gaussian radii R_{out} , R_{side} , and R_{long} , of the pion emission source extracted in this study show a simple scaling pattern

as a function of the characteristic transverse length scale, \bar{R} .

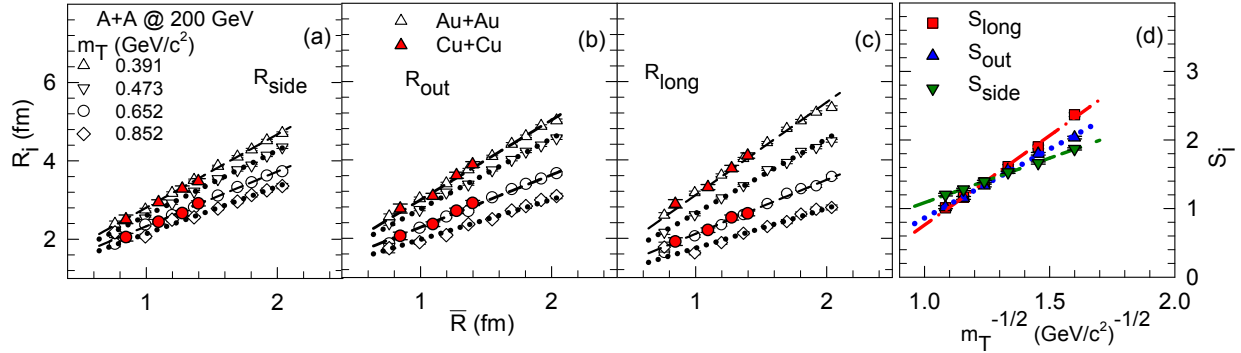


Figure 1.2: Scaling of HBT results with the characteristic length scale, \bar{R} .

Combinations of the three-dimensional radii can be constructed that are sensitive to the medium expansion velocity and lifetime. These observables demonstrate nonmonotonic dependence on $\sqrt{s_{NN}}$, consistent with a softened equation of state, as would be expected near a critical end point in the phase diagram for nuclear matter. These results, shown in Figure 1.3, provide strong constraints on dynamical models of the medium and potential impacts from the QCD equation of state.

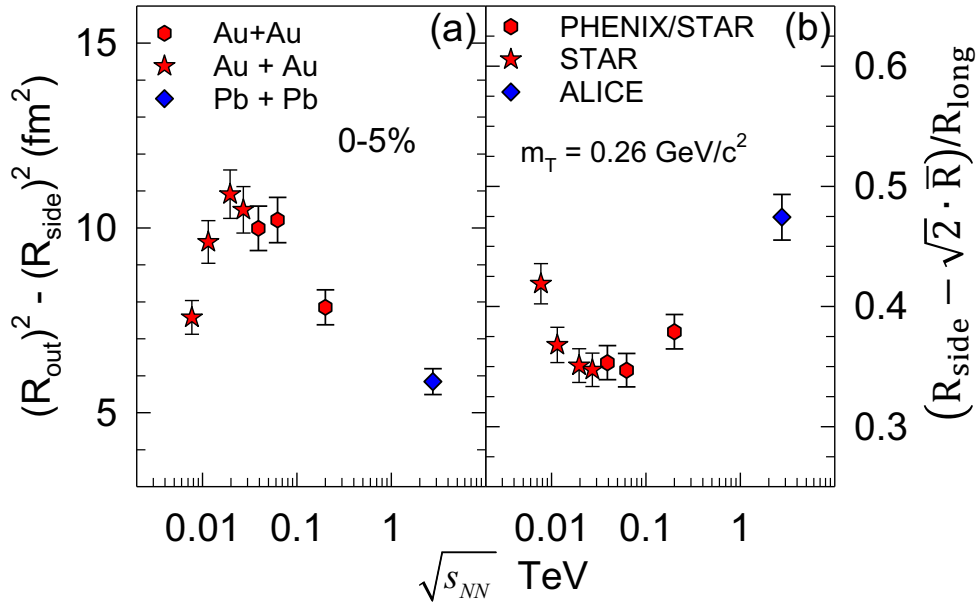


Figure 1.3: Nonmonotonic behavior of HBT radii with $\sqrt{s_{NN}}$.

PHENIX recently published results on the scaling behavior of transverse energy in $p+p, d+Au$ and $Au+Au$ at 200 GeV [7]. The $dE_T/d\eta$ distributions have been compared with the number of nucleon participants N_{part} , the number of binary collisions N_{coll} , and number of constituent-quark participants N_{qp} , each calculated from a Glauber model based on the nuclear geometry.

While $\langle dE_T/d\eta \rangle / N_{\text{part}}$ increases with N_{part} in Au+Au collisions, $\langle dE_T/d\eta \rangle / N_{\text{qp}}$ is approximately constant. This indicates that the two-component ansatz, $dE_T/d\eta \propto (1-x)N_{\text{part}}/2 + xN_{\text{coll}}$, is a proxy for N_{qp} . The $dE_T/d\eta$ as a function of N_{qp} for energies 62.4–200 GeV is shown in Figure 1.4. PHENIX preliminary results indicate that this N_{qp} scaling breaks down at lower collision energies. The results on E_T and $dN_{\text{ch}}/d\eta$ are being prepared for publication.

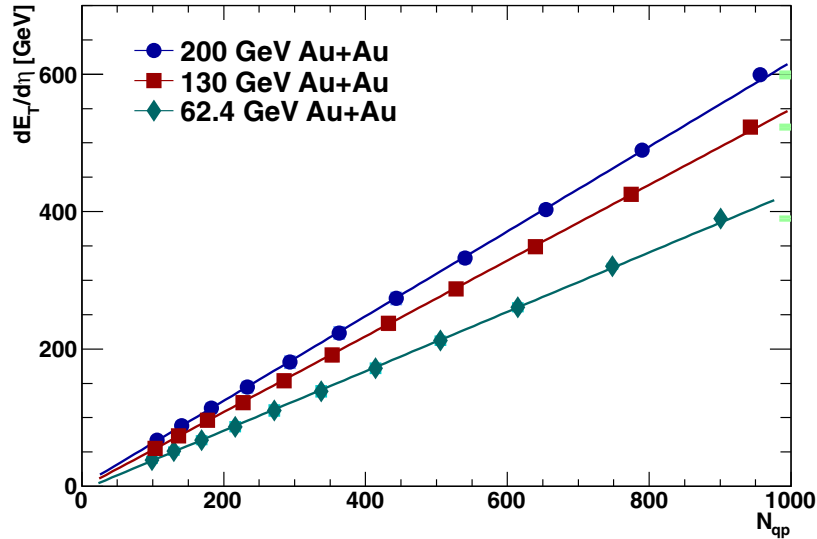


Figure 1.4: $dE_T/d\eta$ as a function of the number of quark participants for Au+Au collisions at $\sqrt{s_{NN}} = 200, 130,$ and 62.4 GeV. The Type A uncertainties are represented by error bars about each point. The Type B uncertainties are represented by error bands about each point shown. The Type A and Type B uncertainties are typically less than the size of the data point. The Type C uncertainties are represented by the error bands to the right of the most central data point. The lines are straight line fits to the data.

The Collaboration has just completed an analysis of unidentified charged particle fluctuations using data covering the full energy range 7.7–200 GeV. This manuscript is currently in internal review and will be submitted soon. Despite the smaller PHENIX acceptance compared to that of STAR, the very high statistics data sets and alternative methodologies will make these results quite impactful. These interesting results underscore the importance of the proposed small-system Beam Energy Scan — detailed in Section 3.4.

1.3 Characterizing the QGP

The PHENIX Collaboration continues to characterize the quark-gluon plasma in full energy Au+Au collisions. In particular, as models of pre-equilibrium dynamics, hydrodynamics with shear and bulk viscosities, and hadronic cascade late stages are refined, data to constrain these different contributions are necessary.

PHENIX recently completed a systematic characterization of charged pion and kaon interferometry in Au+Au collisions at $\sqrt{s_{NN}} = 200$ GeV [8]. At the same m_T , the kaon source radii are found to be

larger than pion radii. This difference increases for more central collisions. The azimuthal-angle dependence of the radii with respect to the second-order event plane for pions and kaons were found to be similar. Hydrodynamic models qualitatively describe the oscillations of the mean source radii for pions and kaons, but they do not fully describe the transverse-mass dependence of the oscillations. A compilation of the behavior of the HBT parameters is shown in Figure 1.5.

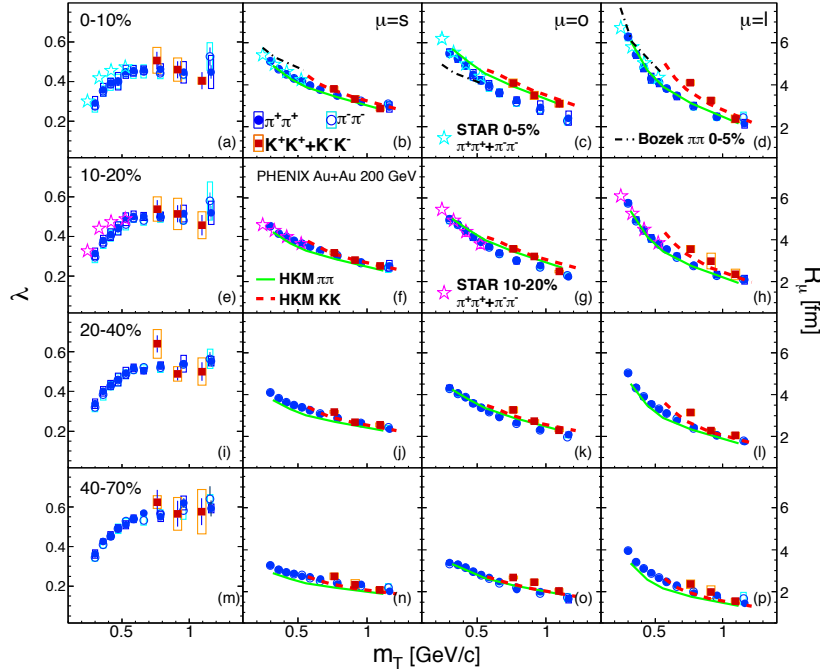


Figure 1.5: Detailed HBT parameter characterization as measured via pion and kaon correlations.

In addition, the Collaboration is finalizing results on the v_2 and v_3 of direct photons in Au+Au collisions at 200 GeV — shown in Figure 1.6. These results significantly extend our previously published results of the surprisingly large v_2 of direct photons [9]. It has remained a challenge to theoretical pictures to simultaneously describe the enhanced yields of direct photons evident in Au+Au collisions and the observed v_2 values. The new results reinforce the existing ones through the use of a different method — external conversions — to obtain v_2 and also by providing the first measurement of direct photon v_3 in Au+Au. Publication of these results is forthcoming.

The Collaboration is working to extract direct photon yields in Au+Au collisions at 39 and 62.4 GeV, from data taken in Run-10. There are now alternate theoretical pictures that favor enhanced medium coupling near the transition temperature T_c . One consequence of that stronger coupling could be increased direct photon yield [10]. PHENIX will soon have results on direct photon yields in Au+Au at 62.4 GeV. Again, these measurements directly inform the Beam Use Proposal, underscoring the need for a larger Au+Au at 62.4 GeV data set and the necessary $p+p$ baseline measurement — see Section 3.3.

A key focus of the recent PHENIX detector upgrades — the silicon VTX and FVTX — is the extraction of open heavy flavor observables. The Run-11 Au+Au data set has been completed produced, and the Au+Au separation of charm and beauty single electrons analysis is now being

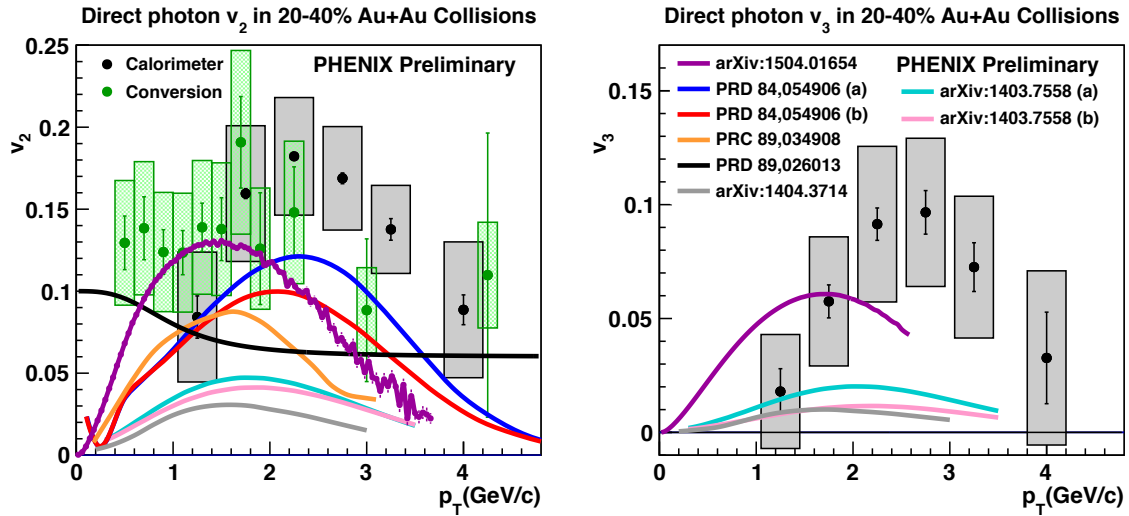


Figure 1.6: Preliminary measurements of direct photon v_2 and v_3 in Au+Au compared to several theory calculations, showing the current tension between simultaneous descriptions of the direct photon yields and their azimuthal anisotropy.

finalized. We expect to submit these results for publication this summer. Similarly, Run-12 Cu+Au FVTX results are being finalized. The Run-14 Au+Au data set is the Golden Data set for these analyses with very high statistics and good detector performance. That production is already well underway.

The performance status of the FVTX and VTX are given in Sections 2.1 and 2.2. Here we highlight that the FVTX is also effective at improving the measurement of heavy quarkonia. Figure 1.7 shows a reconstructed dimuon mass spectrum from Run-13 $p+p$ data using the FVTX and muon detectors. With the FVTX a clear separation of J/ψ and $\psi(2S)$ peaks is obtained and the combinatorial background is reduced as the FVTX detector rejects hadronic backgrounds. Figure 1.7 is the extracted $J/\psi:\psi(2S)$ ratio using the same data, compared to world data.

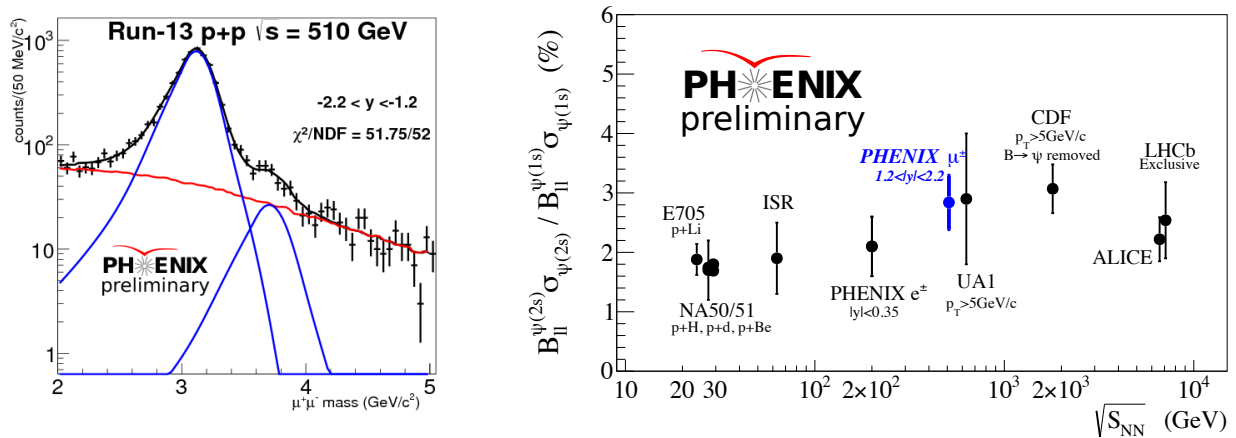


Figure 1.7: The Run-13 $p+p$ unlike-sign mass spectrum showing the J/ψ and $\psi(2S)$ peaks, along with the fits to the two mass peaks and the background.

1.4 Spin Physics

A long standing program for the PHENIX Collaboration is the measurement of large parity-violating single spin asymmetries of high transverse momentum leptons from W^\pm/Z decays, produced in longitudinally polarized $p+p$ collisions at center of mass energies of $\sqrt{s} = 500$ and 510 GeV. These asymmetries allow direct access to the anti-quark polarized parton distribution functions due to the parity-violating nature of the W-boson coupling to quarks and anti-quarks.

The analysis in the electron/positron channel at midrapidity is now complete and the results submitted for publication [11]. The final PHENIX results based on data collected in 2011, 2012, and 2013 with an integrated luminosity of 240 pb^{-1} are shown in Figure 1.8. These results in terms of integrated luminosity exceed previous PHENIX published results by a factor of more than 27. These high Q^2 data provide an important addition to our understanding of anti-quark parton helicity distribution functions. The analysis of the muon channel at forward rapidity is ongoing. Preliminary results from the full Run-13 $p+p$ at 510 GeV data set were shown in 2014 [12], and additional systematic checks are being completed to finalize the results.

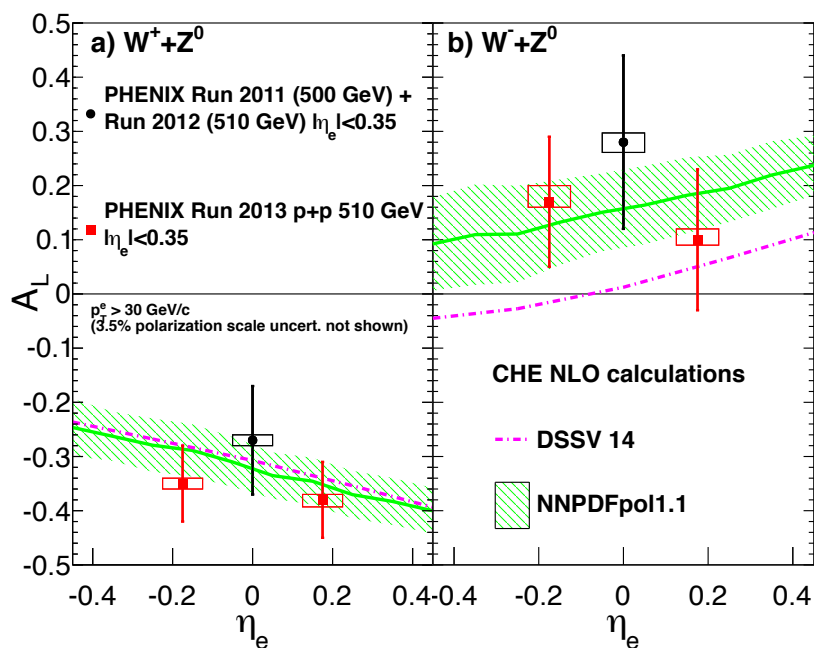


Figure 1.8: Asymmetry results from the combined 2011 and 2012 data sets for $|\eta| < 0.355$ (black circles) and the 2013 data (red squares) separated into two equal η bins between -0.35 and 0.35. The green line and shaded region shows a theoretical calculation using CHE with the NNPDFpol1.1 PDF sets, while the dashed magenta line shows the DSSV14 calculation.

There has been a great deal of excitement recently about the new constraint on ΔG , utilizing high statistics PHENIX and STAR results. New results on the PHENIX π^0 double spin asymmetry from $p+p$ at 510 GeV form a significant contribution to a global fit that indicate for the first time a non-zero value for ΔG . Figure 1.9 shows the PHENIX results for double spin asymmetries at both 200 and 510 GeV. While the 200 GeV results are compatible with $A_{LL} = 0$, the new higher \sqrt{s} data

lies significantly above zero. The net result of all the world data in a global fit is a non-zero value of ΔG . The Collaboration is finalizing these results and expects to submit them for publication this summer.

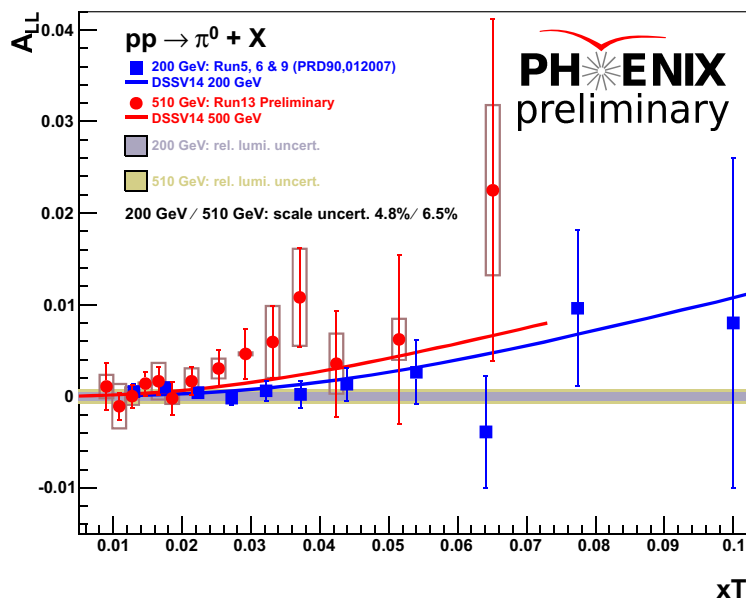


Figure 1.9: A_{LL} vs. x_T for 510 GeV and 200 GeV data. DSSV14 theory curves are also shown. The boxes on the red 510 GeV A_{LL} points show the systematic uncertainty from the discrepancy of two independent analysis. Gray and yellow bands are systematic uncertainties from relative luminosity. Both the experimental data and theory curves favor a non-zero A_{LL} .

1.5 Beyond the Standard Model

The Collaboration has finalized and published a limit on the coupling between a possible “dark photon”, U , and the usual QED photon. The dark photon has been seen as a possible explanation of the 3.6σ discrepancy between the measured value of the muon anomalous magnetic moment $(g - 2)_\mu$ and SM calculations. PHENIX searched for a dark photon signal in $\pi^0, \eta \rightarrow \gamma e^+ e^-$ Dalitz decays and obtained upper limits for U - γ mixing at 90% C.L. for the mass range $30 < m_U < 90 \text{ MeV}/c^2$. When combined with other experimental limits [13, 14], these results essentially eliminate a minimally coupled dark photon as an explanation of the $(g - 2)_\mu$ anomaly, and they significantly inform future dark photon searches, including by the PHENIX Collaboration.

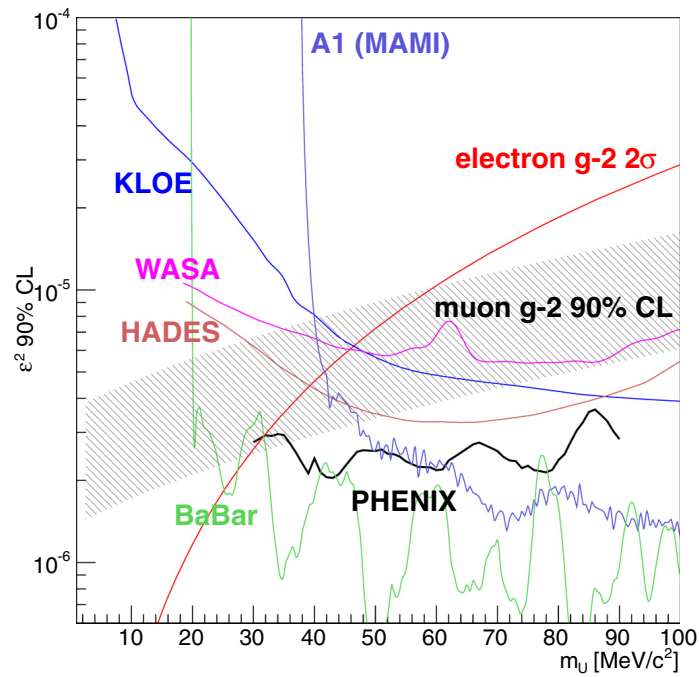


Figure 1.10: A compilation of the limits on the U - γ mixing parameter, showing the PHENIX results. Also shown are the limits at 90% C.L. from WASA, HADES, KLOE, A1(MAMI), and BABAR experiments and the band indicating the range of mass and coupling parameters favored by the $(g-2)_\mu$ anomaly at 90% C.L. Also shown is the 2σ upper limit obtained from $(g-2)_e$.

Chapter 2

Status of upgrades

In this Chapter we report on the status of key PHENIX detector upgrade projects. The first two sections relate to the forward silicon vertex detector (FVTX) and the the barrel silicon vertex detector (VTX), which are particularly relevant to the proposed data taking in 2016. We also include an update on the Muon Piston Calorimeter Extension upgrade (MPC-EX) that was installed just prior to Run-15, and is a key part of that physics program.

2.1 Forward silicon vertex detector (FVTX)

The PHENIX detector Barrel and Forward Silicon Vertex Trackers are shown in Figure 2.1. The two Forward Silicon Vertex Trackers (FVTX), which are described elsewhere in detail [15], are endcap detectors which extend the vertex capability of the VTX to forward and backward rapidities, providing space points before the absorber materials and secondary vertex measurement capability in front of the PHENIX muon arms. The FVTX detector was successfully installed into PHENIX in December 2011 and has undergone commissioning and operations during RHIC Runs 12–15. The FVTX detector has maintained an operational state of $>95\%$ live channels and the intrinsic performance of the FVTX detector has been established to be $>95\%$ efficient in the active area, ~ 500 electrons noise level on all readout channels, and an intrinsic detector resolution limited only by the readout pitch and multiple scattering of particles.

The FVTX was designed to identify secondary vertices near the primary event vertex. With a distance of closest approach (DCA) resolution of better than $200 \mu\text{m}$ at $5 \text{ GeV}/c$, we can separate prompt particles from particles that have short decay distances (B and D mesons) and longer-lived particles such as pions and kaons. The FVTX detector improves the dimuon mass resolution by providing a better opening angle measurement than is available from the muon arms alone, enables isolation cuts to help discriminate between muon signals and hadronic backgrounds, and provides further discrimination against hadronic particles which decay in the muon volume by requiring that the track passing through the FVTX planes and the muon planes have a good χ^2 fit value. With these added capabilities, we can precisely measure open heavy flavor production at forward rapidity, improve the background rejection and separation of J/ψ and $\psi(2S)$ in the dimuon spectra, and separate Drell-Yan dimuons from dimuons produced through heavy flavor and/or hadronic

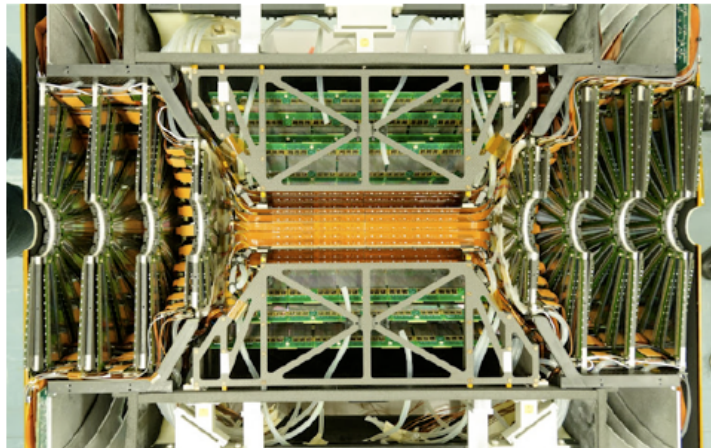


Figure 2.1: Photograph of VTX barrel plus FVTX end cap.

decays. The FVTX detector also improves the reaction plane measurement significantly and is providing a new precision measurement of the relative bucket-to-bucket luminosities in polarized $p+p$ collisions, which is critical for PHENIX spin analyses.

Vector meson analyses with the Muon arms and the FVTX from Runs 12–14 are underway. In addition to the J/ψ and $\psi(2S)$ yields shown in earlier in Figure 1.7, J/ψ and $\psi(2S)$ peaks for the Run-12 Cu+Au data have also been extracted, as shown in Figure 2.2, and work is underway to extract the same $J/\psi:\psi(2S)$ ratios for the Cu- and Au-going directions, to look for cold and hot nuclear matter effects on the ratio. In addition to extraction of the J/ψ and $\psi(2S)$ yields, we are working to measure the production as a function of the event multiplicity, both to see whether the relative modification of the ratio continues to follow a common trend versus $dN/d\eta$ as shown in Ref. [16] and also to compare the $p+p$ production versus particle multiplicity to the recent ALICE results [17] which may indicate multi-parton interactions in $p+p$ collisions. The latter measurement also requires that in $p+p$ at 510 GeV running we clearly separate multiple interactions in a given event from each other, and the FVTX detector has been established to be able to do this with high accuracy.

To achieve the DCA resolution needed to separate heavy flavor decays from hadronic backgrounds, much work has gone into achieving precise alignment within the FVTX and VTX detectors and between the two. As a result we are now able to extract DCA resolutions that are very similar to those obtained in simulations. An example of the DCA that is measured for muons nominally coming from J/ψ decays is shown in the left panel of Figure 2.3 where the DCA distribution for J/ψ candidates is shown for the Run-12 Cu+Au data for high momentum tracks, and the extracted resolution versus momentum for the same data set compared to Monte Carlo calculations is shown in the right panel.

The FVTX detector also now provides the highest precision event planes from the existing PHENIX detectors and is an integral part of forward rapidity flow analyses. FVTX clusters were used in the second- and third-order event plane determination in the Run-14 $^3\text{He}+\text{Au}$ collisions at $\sqrt{s} = 200$ GeV, as shown earlier in Figure 1.1. Compared with the traditional Beam-Beam Counter

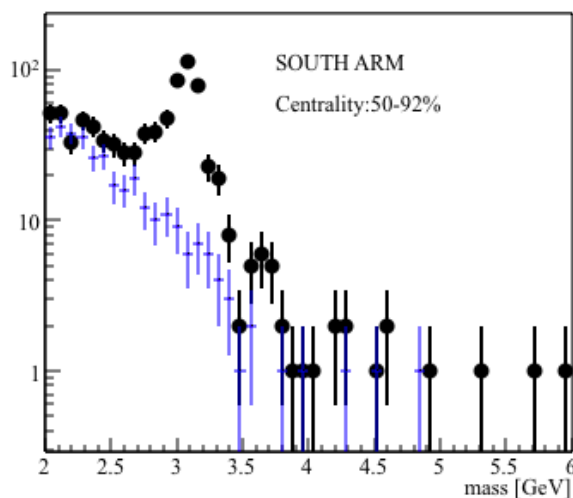


Figure 2.2: A Run-12 Cu+Au unlike-sign mass spectrum for the South Arm showing the J/ψ and $\psi(2S)$ peaks, along with combinatorial background represented by the like-sign distribution (blue points).

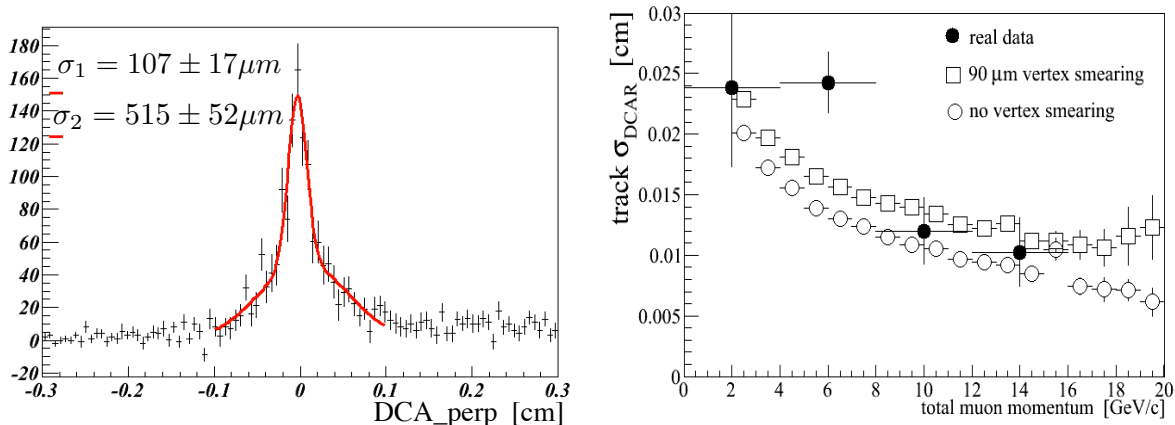


Figure 2.3: The DCA resolution extracted from Run-12 Cu+Au data (left-hand plot) and from Run-12 Cu+Au data vs momentum, compared to Monte Carlo (right-hand plot). For both plots, muons nominally originating from J/ψ decays were selected.

(BBC) and Muon Piston Calorimeter (MPC) based event planes, the FVTX improves the resolutions by roughly a factor of two. The $^3\text{He}+\text{Au}$ flow measurements using the FVTX event planes will contribute an essential piece of information to the global effort in separating the flow contributions from the initial geometry and medium evolution. We expect to use similar approaches in the coming Run-15 $p+\text{Au}$ measurements. The FVTX detector directed flow (v_1) in Cu+Au collisions, which helped provide a large rapidity range measurement, is shown in Figure 2.4.

In Run-15, the FVTX has been used to provide a track counting trigger to enhance collection of events with high multiplicity so that we can study whether RHIC sees any indication of collective behavior in $p+p$ and $p+\text{Au}$. An online trigger algorithm was implemented in our readout FPGAs

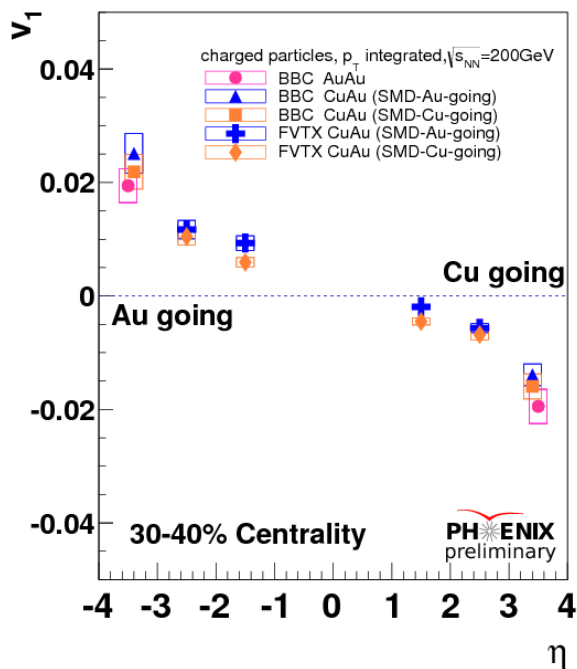


Figure 2.4: Pseudo-rapidity dependence of directed flow, extracted from Run-12 Cu+Au data.

and commissioned at the beginning of the Run-15 $p+p$ run. The correlation of the tracks measured by the trigger with the number reconstructed in offline is shown in the left panel of Figure 2.5 and the turn-on efficiency curve for various trigger configurations is shown in the right-hand side of Figure 2.5. A trigger threshold of 12 tracks per arm was selected for Run-15 $p+p$ running and we recorded our target goal of high-multiplicity events. The alignment of the VTX and FVTX is complete, and that data set is currently being reconstructed for full analysis.

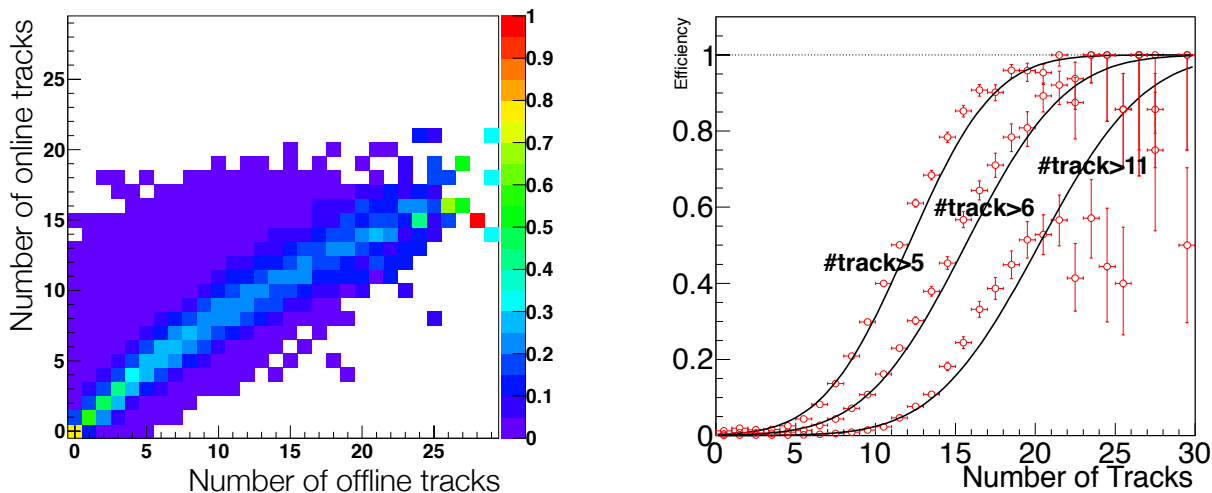


Figure 2.5: The correlation of online tracks measured in an FVTX trigger to offline reconstructed tracks (left) and the trigger efficiency curve versus number of tracks in an event (right).

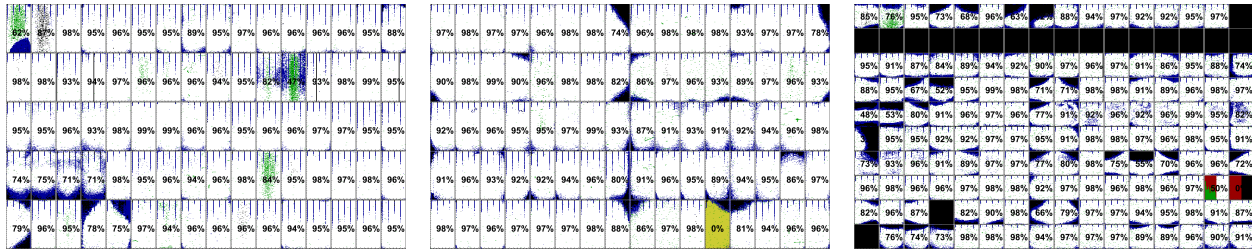


Figure 2.6: Live / Dead / Unstable map of the VTX inner pixel layers.

2.2 Barrel silicon vertex detector (VTX)

The PHENIX barrel silicon vertex detector (VTX) is a four layer silicon tracker. The inner two layers, B0 and B1, are made of pixel detectors and the outer two layers, B2 and B3, are made of stripixel detectors. The VTX detector was installed in the PHENIX interaction region in December, 2010 and had its first commissioning with beam and data taking in Run-11.

During Run-11, the detector had issues with the read-out electronics for the pixel system. As a result, many of the pixel ladders were not properly read-out, which reduced the live area of the detector during the run. This problem was repaired during the shutdown after Run-11. Additionally, some of the pixel ladders were damaged in the time frame of Run-11. Wire-bonding between the pixel sensors and the read-out buses were broken. The cause of the damage was not completely understood, but the most likely cause was thermal stress. The problem has been addressed through an extensive two-year repair program and an improvement to the operating condition of the VTX that minimizes large changes to the operating temperature of the ladders. No damage of any significance has occurred to the pixel ladder wire bonds during from Run-12 up to the present time in Run-15. The repair program involved the removal of all damaged pixel ladders from the VTX, re-bonding of these damaged ladders, and re-installing those repaired ladders into the VTX. We also installed spare ladders with improved performance. The repair program was complete ahead of the start of Run-14. The live area performance of the pixels has been quite stable throughout Run-14 and the current Run-15. A typical snapshot of the live area is shown in Figure 2.6. The main limitation on the live area is determined by bump-bond problems in the corner regions that are from the thermal stress problems during the Run-11 data taking.

The stripixel detectors had minor read-out issues in Run-11 and Run-12 and those issues were addressed during the shutdown after each run. However, just prior to Run-13, the cooling tubes of the stripixel detector developed multiple, severe coolant leaks. The leaks were caused by galvanic corrosion of the aluminum tube. We designed and built new staves without aluminum material and rebuilt all 40 stripixel ladders by moving the silicon sensor modules from old staves to new staves. This repair program was very successful and was complete prior to the start of Run-14. The newly rebuilt VTX detector was installed in the PHENIX interaction region for Run-14. The repairs were successful. The performance of the stripixel in Run-14 was relatively stable, though with a problems due to condensation in the cooling system towards the end of Run-14 Au+Au data taking and the following $^3\text{He}+\text{Au}$ running. Run-15 performance has been good. These bump-bond problems appear to be stable, i.e. not deteriorating and beyond those only one ladder in B1 shows a communication error.

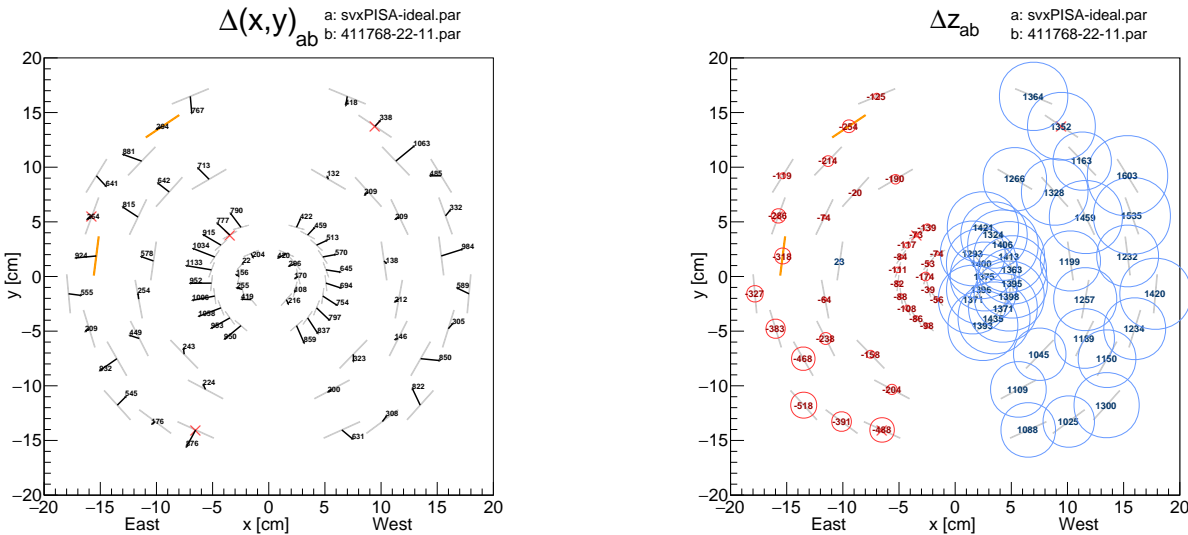


Figure 2.7: We have developed a new VTX alignment method using the Millipede II package. This results in a convergent simultaneous alignment.

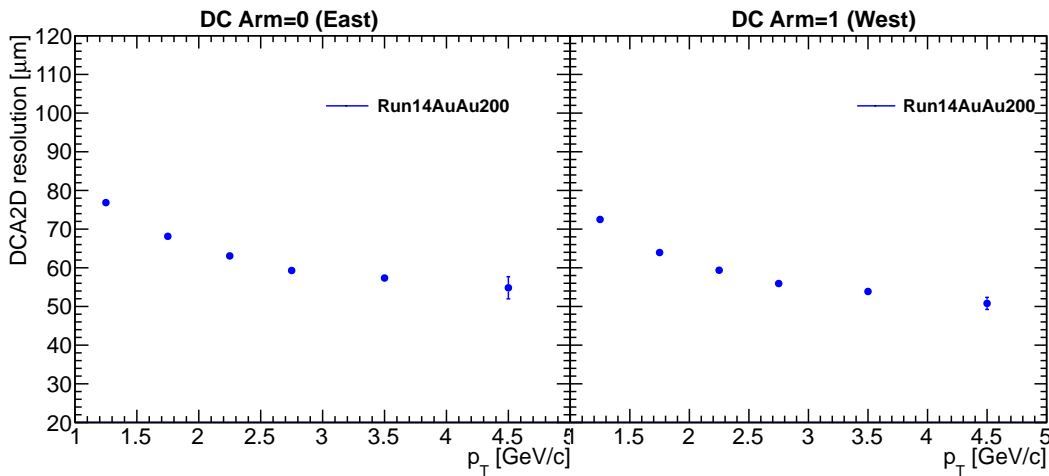


Figure 2.8: DCA resolutions that have exceeded the detector performance specifications – in Au+Au collisions from Run-14.

In the last year, a new Millipede-based alignment has been developed and employed [18]. The results allow for a convergent procedure for aligning the VTX ladders as a single unit from zero magnetic field running. Then a global relative alignment is performed to the PHENIX outer central arm detectors. For Run-15, the alignment was complete within two days of a zero magnetic field run. The procedure is visually highlighted in Figure 2.7 and the distance of closest approach (DCA) performance is shown in Figure 2.8. The DCA performance utilizing this alignment procedure exceeds the original design specifications.

We are close to finalizing the Run-11 Au+Au data analysis, which has been challenging due to

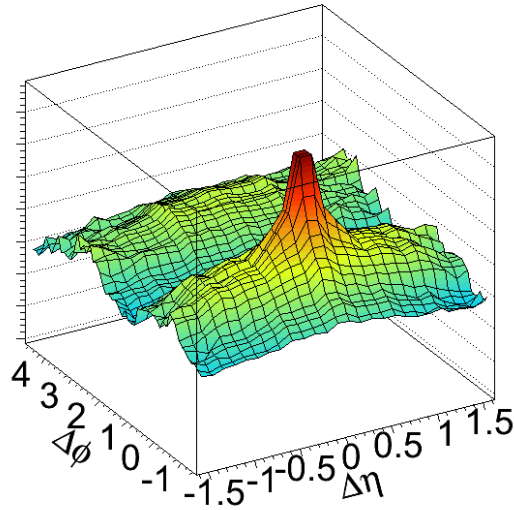


Figure 2.9: New physics enabled by extended pseudo-rapidity coverage with VTX only tracking. Result in central 0-5% $^3\text{He}+\text{Au}$ collision at 200 GeV from Run-14.

the initial detector issues described above. A PHENIX Paper Preparation Group (PPG) has been formed and the final results should be in publication form shortly. The Run-12 Cu+Au data set has been reconstructed and analysis is ongoing.

The Run-14 Au+Au data looks to be of very high quality and should provide our golden data set of open heavy flavor physics when combined with the projected high statistics Run-15 $p+p$ at 200 GeV running as the baseline. The Run-14 Au+Au data production is 25% complete and ongoing. We note that the Run-14 $^3\text{He}+\text{Au}$ data set has already been completely reconstructed. The VTX is primarily designed for the heavy flavor DCA analysis, but can also reconstruct tracks without the outer PHENIX central. This gives PHENIX a large pseudo-rapidity coverage for unidentified charged hadrons. Using such tracks, we highlight from $^3\text{He}+\text{Au}$ 0-5% central events the two-particle correlation in $\Delta\phi$ and $\Delta\eta$ space. The near-side long-range ridge correlation is directly observed in $^3\text{He}+\text{Au}$ collisions using the VTX alone.

2.3 Muon piston calorimeter extension (MPC-EX)

The Muon Piston Calorimeter (MPC) Extension, or MPC-EX, is a silicon-tungsten preshower detector installed in front of the existing PHENIX MPCs, as shown in Figure 2.10, for Run-15. This detector consists of eight layers of silicon “minipad” sensors interleaved with tungsten absorber and enables the identification and reconstruction of prompt photons and π^0 s at energies up to ~ 80 GeV.

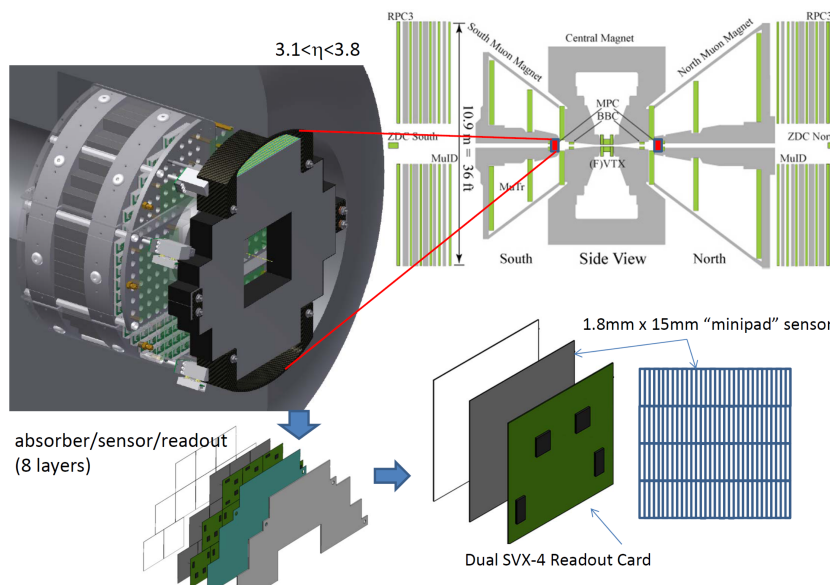


Figure 2.10: The PHENIX detector (upper right), showing the location of the existing Muon Piston Calorimeters inside the muon magnet piston. The MPC-EX (upper left) consists of eight measurement layers of absorber, sensors and readout. The “minipad” sensors themselves (lower right) will consist of a readout card bonded to a Si sensor. The orientation of the long direction of the minipads alternates between layers.

The MPC and MPC-EX sit at forward and backward rapidities ($3.1 < |\eta| < 3.8$) and are uniquely positioned to measure phenomena related to either low- x partons (in the target hadron or nucleus) or high- x partons (in the projectile nucleon or nucleus). We are using the MPC-EX to make critical new measurements that will elucidate the gluon distribution at low- x in nuclei as well as the origin of large transverse single spin asymmetries in polarized $p+p$ collisions.

The MPC-EX was installed in both PHENIX arms prior to Run-15, and both detectors were commissioned and operational by March 17, 2015. The north detector had approximately 90% live channels, with the 10% loss in channels arising from a problem in the SVX4 readout at particular locations on the SVX4 readout chain on each carrier board. This problem is under investigation in bench tests, and we hope to be able to address this issue between Run-15 and Run-16 and recover the lost channels. In addition, after installation we were unable to program the south MPC-EX top carrier board for layer-10 with new firmware, resulting in a loss of an additional 10% of channels in the south arm. The loss of the top layer 0 in the south is not considered particularly important, as the electromagnetic shower is just starting to develop after the first layer of tungsten. This issue can be addressed and south top layer 0 can be recovered between Run-15 and Run-16.

At the time of this writing, the $p+p$ running period has completed, and the MPC-EX successfully sampled 52 pb^{-1} within a vertex limit of 40 cm, slightly more than the goal of 50 pb^{-1} . This data was sampled with a high-tower trigger in the MPC designed to collect high $p_T > 3 \text{ GeV}/c$ momentum electromagnetic showers from π^0 s and prompt photons. Figure 2.11 shows that in MPC high-tower trigger events MPC-EX showers are well-matched to high energy clusters in the MPC, demonstrating that the MPC and MPC-EX data are well correlated and timed to the same beam crossing.

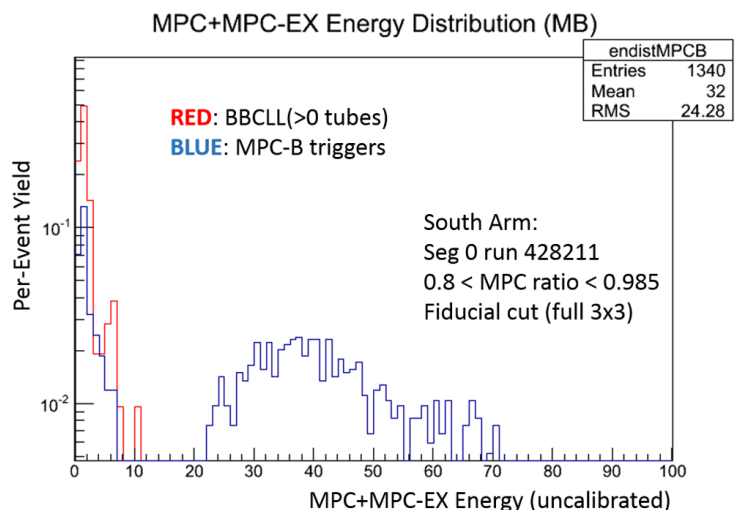


Figure 2.11: Per-trigger yields of combined MPC-EX showers with MPC clusters for minimum bias triggers (BBCLL1) and MPC high-tower triggers (MPC-B). The overall energy scale is uncalibrated. This plots shows that in MPC high-tower trigger events, combined MPC-EX/MPC objects are found with high energy, as expected.

Calibration of this new detector system is ongoing and we expect to be able to give a complete report by the time of the PAC meeting in June 2015. As an example of the quality of the data and ongoing calibrations, Figure 2.12 shows the pedestal-subtracted ADC spectra for MPC-EX high-gain minipads. A clear signal of minimum ionizing particles is clearly evident in the data, at the location expected from bench tests with cosmic muons. The location of the MIP peak in the MPC-EX high-gain ADCs will be used to calibrate the energy scale for the detector and monitor variations in the gain over time. The high-gain ADCs will be used for the high-energy π^0 reconstruction.

The second component of the calibrations involves the ratio between the high and low-gain ADC channels in each micromodules. The charge split is provided by a set of small capacitor arrays whose capacitance varies, so the charge split must be measured for groups of channels. Figure 2.13 shows an example of the high/low ADC ratio in south layer 4. The MIP location in the high-gain ADCs combined with the H/L ratio allows calibration of the low-gain minipad ADCs, which will be used for the overall energy measurement from the MPC-EX.

The Collaboration has worked very hard to have the detector installed and taking physics data in Run-15. The MPC-EX team is energized to analyzing the data in a timely fashion and learning the physics answers.

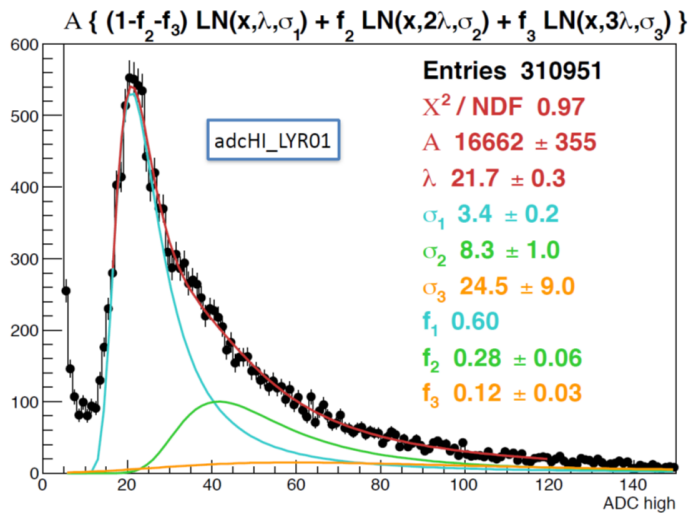


Figure 2.12: Pedestal subtracted minipad high-gain ADC spectra for minimum bias events. A clear signal from minimum ionizing particles can be seen. Minimum ionizing particles will be used to calibrate the energy scale in the MPC-EX high-gain minipads.

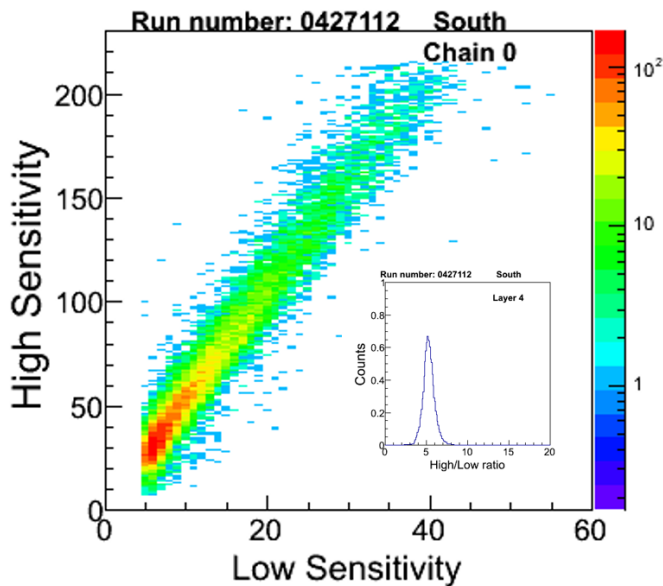


Figure 2.13: Correlation between high and low-sensitivity ADC spectra in the MPC-EX minipads. The inset shows a histogram of the H/L ratio extracted from all minipads in the south layer-4 minipads. The calibration of the H/L ratio, combined with the high-gain MIP ADC values, will be used to set the scale for the MPC-EX low-gain minipads.

Chapter 3

Proposal for Run-16

In this section we provide details on the PHENIX collaboration beam use request, including the assumptions and inputs for luminosities and number of weeks for each request.

3.1 Accelerator performance and luminosity estimates

The physics performance evaluations in this document are based upon guidance provided by the Collider-Accelerator Department (C-AD) as documented in Ref. [19]. Also necessary are projections for the PHENIX experiment performance in terms of uptime and trigger sampling. We use the following values based on metrics from the recent experimental runs.

- The PHENIX uptime (the fraction of time when the beams are colliding that the PHENIX data acquisition is running and thus sampling physics) is 70%. This has been an area that PHENIX has placed particular emphasis on and observed consistent improvement.
- The PHENIX forward and barrel silicon vertex detectors have an optimal acceptance for collisions with z -vertex $|z| < 10$ cm. For other analyses in the central arm spectrometers not requiring the vertex detectors the acceptance is optimal for $|z| < 30$ cm. We have labeled all physics projection integrated luminosities with the corresponding z -vertex range. For the Au+Au at 200 GeV, we assume that 60% of all collisions are within $|z| < 30$ cm, and 30% of all collisions are within $|z| < 10$. The lower energy proposed running has a wider z -vertex distribution and lower percentages, that are documented in the relevant section.
- The PHENIX data acquisition livetime is quite high — typically better than 90%.

All of this information is used and the values quoted in the performance figures are in terms of sampled integrated luminosity by PHENIX within the specified z -vertex range.

3.2 Run-16 Au+Au at 200 GeV Running

In the report from the NPP Program Advisory Committee in 2014 [20], the clear recommendation as “highest priority” was for 10 physics weeks of running for Au+Au at 200 GeV. Thus, we have incorporated that into the PHENIX Collaboration Beam Use Proposal, though it does not represent the optimal physics data taking with PHENIX considerations alone.

The Run-14 Au+Au at 200 GeV run was extremely successful (as shown in Figure 3.1) and resulted in recording 2.3 nb^{-1} , equivalent to 14.2 billion minimum bias events within a z -vertex range $|z| < 10 \text{ cm}$. This substantially exceeds our original Run-14 beam use request of 1.5 nb^{-1} . This great success is due to the fantastic performance of RHIC and the C-AD team, and a very efficient data taking and high live time for the PHENIX experiment. The silicon vertex barrel and forward detectors operated successfully throughout Run-14 with high efficiency and good acceptance. Our data acquisition ran at high rate and recorded (not just sampled) approximately 85% of all collisions within that z -vertex range when we were taking data. The steady high luminosity long stores delivered have also resulted in very high data taking efficiency as shown in Figure 3.2. The Run-14 data sample when combined with the recently completed Run-15 $p+p$ at 200 GeV data sample represent our Golden Data Set for the study of open heavy flavor with the silicon detectors.

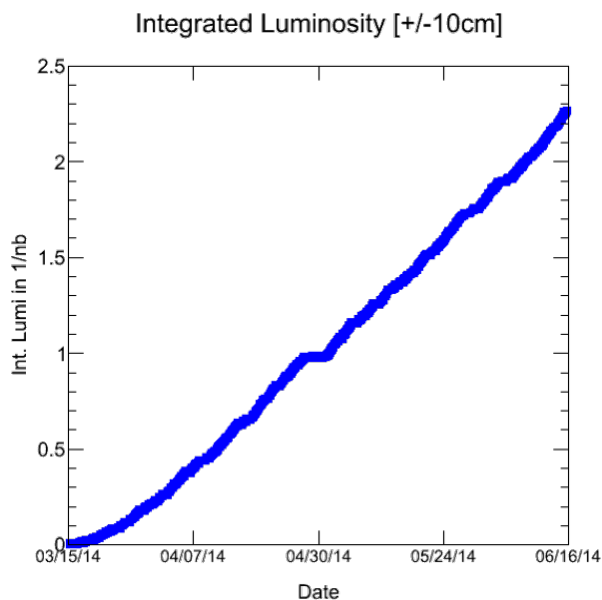


Figure 3.1: Run-14 Au+Au at 200 GeV integrated luminosity as a function of day during the run.

Here we address the physics potential for PHENIX of this Au+Au at 200 GeV running in Run-16. Note that the PHENIX detector will have essentially the same capabilities and acceptance as the Run-14 data taking (with the exception of the MPC-EX which operates only in lower occupancy $p+p$ and $p+A$ collisions).

The Run-14 beam conditions had a somewhat wide z -vertex distribution, including satellite peaks as shown in Figure 3.3. From this typical distribution, one finds that 23% of all collisions occur within the optimal acceptance of the silicon detectors $|z| < 10 \text{ cm}$, and 51% within $|z| < 30 \text{ cm}$. If one excludes the satellite peaks, these values increase to 36% and 84% respectively. If the 56 MHz

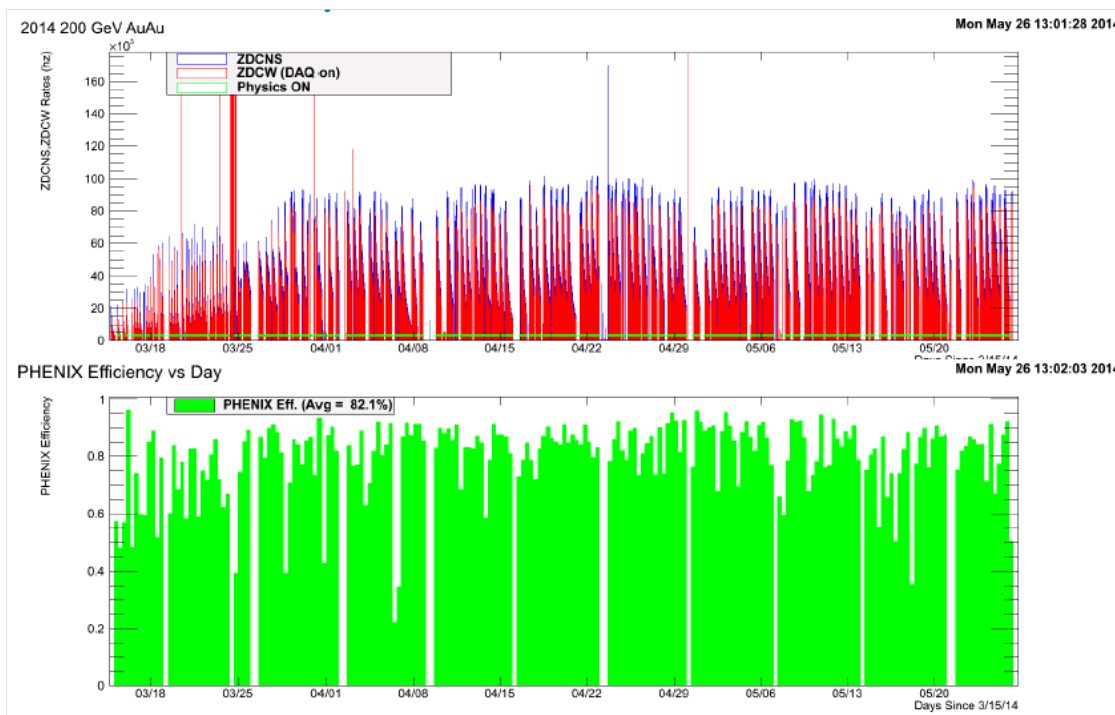


Figure 3.2: Graphical summary of the run performance for stores delivered and PHENIX data taking efficiency.

RF would be successful at capturing these satellite peaks into the main distribution, one could get a 50% increase in the rate within the tighter required z -vertex range. There are other optimizations being explored with C-AD that might result in slightly higher overall collision rates. These could be sampled with some increase in PHENIX data acquisition bandwidth (that might be achievable with some Event Builder upgrades and re-configuration), in addition to higher transverse momentum electrons and photons utilizing our ERT trigger.

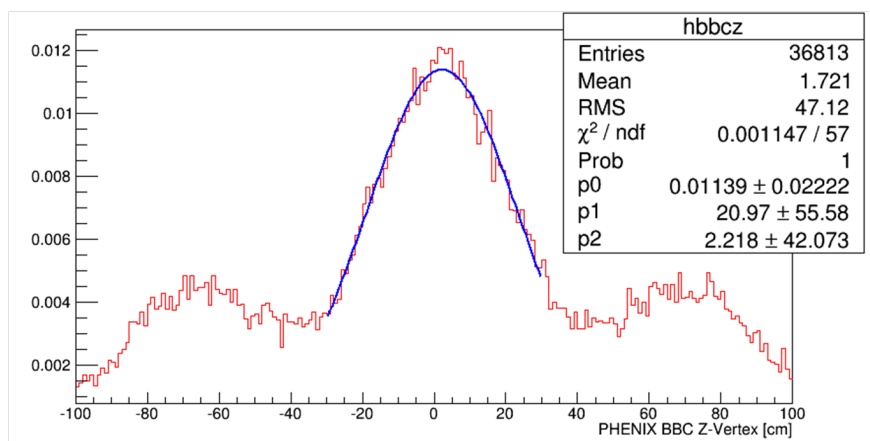


Figure 3.3: Run-14 Au+Au z -vertex distribution.

The latest C-AD projections are shown in Figure 3.4, and indicate that even in the maximum

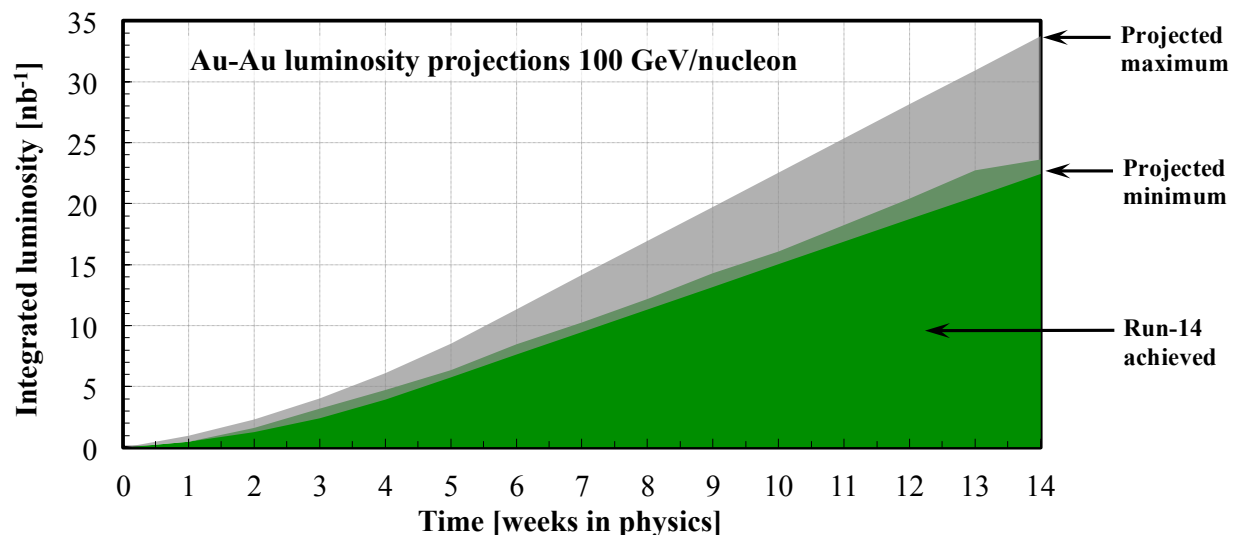


Figure 3.4: Shown are the C-AD projections for integrated luminosity as a function of weeks of physics running.

scenario, one might double the Run-14 data sample.

In an optimistic scenario, a ten-week physics run might result in a data sample comparable to that recorded in Run-14. If analysis of the Run-14 data set reveals particularly interesting results for higher p_T electrons, this factor of two increase in statistics could prove to be insightful. Currently, we project 1.8 nb^{-1} or 12 billion recorded minimum bias Au+Au events within the narrow vertex range. Depending on results from Run-14, one could imagine a balance of more central events or higher p_T triggers that might lead to a modest enhancement in the more interesting data sample — of order 20–50% more.

3.3 Run-16 Au+Au and $p+p$ 62 GeV Program

A unique ability of RHIC is to change the beam energy and thus scan quark-gluon plasma interactions above, near, and below the transition temperature. Recent measurements from our Run-10 Au+Au at 62.4 GeV data set indicate surprising results in the heavy flavor sector [2]. Measurements of open heavy flavor with the PHENIX silicon detectors in this system closer to the transition temperature, and thus potentially stronger early-time coupling, should provide key new information on the quark-gluon plasma and flow of heavy quarks in medium. In addition, the steeper initial p_T spectrum of charm quarks actually makes this probe more sensitive to flow effects.

Figure 3.5 shows the now published PHENIX results on non-photonic electron spectra (measured prior to the installation of the silicon detectors) in Au+Au collisions at 62.4 GeV. The FONLL calculation as the $p+p$ baseline. One observes the Au+Au spectra is above the binary scaled $p+p$ references, i.e. $R_{AA} > 1$. This is shown explicitly in Figure 3.7, where the uncertainties are highly correlated and dominated by the $p+p$ reference. This is strikingly different from measurements in Au+Au collisions at 200 GeV. Preliminary STAR measurements in Au+Au at 62.4 GeV indicate a

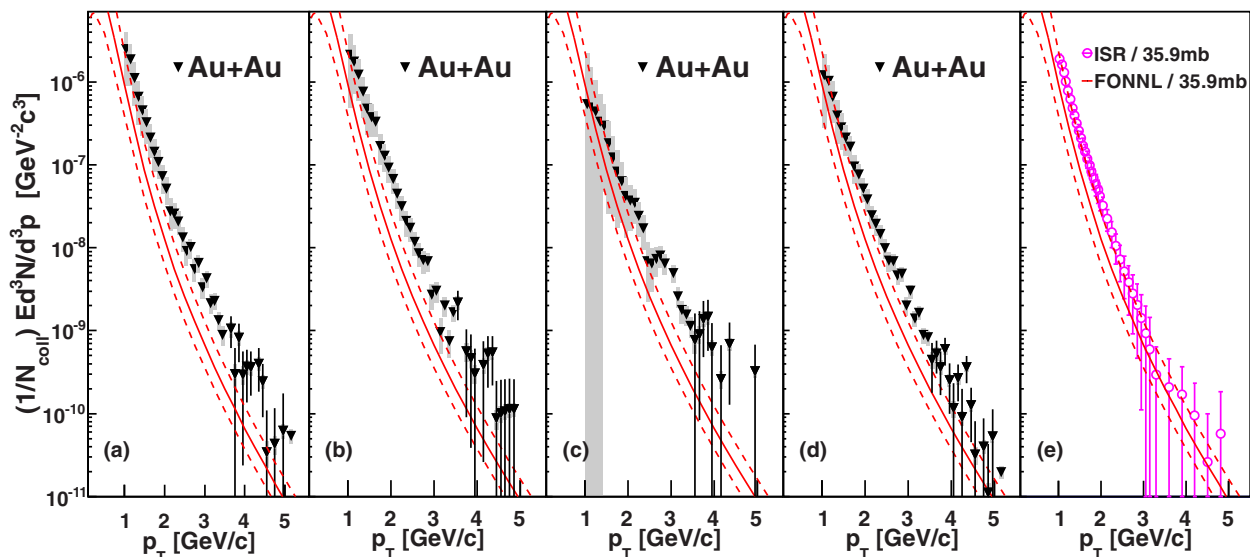


Figure 3.5: Shown are the measured non-photonic electron spectra from Au+Au collisions at 62 GeV for various centralities. In each selection, a comparison with binary scaled reference FONLL calculations are shown, detailed in the right most panel.

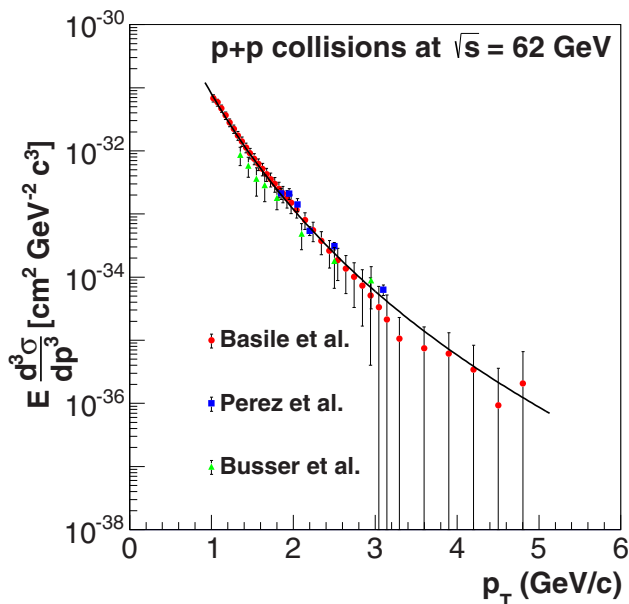


Figure 3.6: Shown are invariant yields of non-photonic electrons from three ISR publications for $p+p$ collisions at 62 GeV.

similar enhancement effect [21]. We note that there is no RHIC measured $p+p$ reference data set and only older ISR measurements exist — as shown in Figure 3.6.

We have received additional guidance from C-AD on running conditions at this energy. Both the storage RF system and stochastic cooling work at this energy. Mike Blaskiewicz simulated the store luminosity for all cases, and the details are given in Table 3.1.

Table 3.1: C-AD providing information on $p+p$, $p+A$, Au+Au running at 62.4 GeV.

Collision System	Luminosity	$L(z < 30 \text{ cm})/L_{\text{tot}}$	$L(z < 10 \text{ cm})/L_{\text{tot}}$
Au+Au @ $\sqrt{s_{NN}} = 62.4 \text{ GeV}$	$400 \mu\text{b}^{-1}/\text{week}$	45%	15%
$p+p$ @ $\sqrt{s_{NN}} = 62.4 \text{ GeV}$	$2.1 \text{ pb}^{-1}/\text{week}$	23%	8%
$p+Au$ @ $\sqrt{s_{NN}} = 62.4 \text{ GeV}$	$20 \text{ nb}^{-1}/\text{week}$	35%	12%

Following our standard running assumptions detailed earlier, for Au+Au at 62.4 GeV this would enable PHENIX to record 1.5×10^9 events within the silicon detector acceptance of $|z| < 10 \text{ cm}$ in a five week running period. In a two week run of $p+p$ at 62.4 GeV, the result would be 1×10^{10} PHENIX trigger sampled events.

In fact, $p+Au$ or $d+Au$ running at 62.4 GeV would be very interesting and key additional constraints on the physics. We do not make it an explicit proposal only due to the constraints on Run-16 asymmetric species (i.e. $p+A$) running and the overall limit on cryo-weeks. If additional running time were available, a short $d+Au$ run at 62.4 GeV would be very interesting (see the alternate proposal for the Small-System Beam Energy Scan in Section 3.4).

Detailed below is a possible run plan for 62.4 GeV data taking. The short set-up time for Au+Au running assumes that this follows the Au+Au run at 200 GeV and C-AD projects a short transition time. The 1.5 week set-up for the $p+p$ running at 62.4 GeV also depends on the polarization performance required for this running. In the physics case presented in this section, all measurements are unpolarized in which case this set-up time might be reduced. We address the issue of utilizing this short running period for polarized $p+p$ physics at the end of this section.

- 0.5 weeks set-up
- 5.0 weeks Au+Au 62.4 GeV data taking
- 1.5 week set-up
- 2.0 weeks $p+p$ @ 62.4 GeV data taking

The above numbers indicate substantial data sets, and for example for Au+Au this would be much larger than the 400 million events from the Run-10 data set (which was prior to any of the PHENIX silicon vertex detectors being installed). These are smaller than data sets at 200 GeV and the total charm cross section is approximately a factor of five smaller at 62.4 GeV collision energy.

Taking all of these factors into account, we show in Figures 3.8 and 3.7 the projected uncertainties on the charm to electron nuclear modification factor R_{AA} , as well as the R_{AA} from RHIC Run-10, compared to a prediction by Rapp *et al.* [22]. We note that the improvement in systematic uncertainties at the lowest p_T is due to the use of the VTX to reject background from photonic electrons, while at high p_T the improvement is mainly due to the improved $p+p$ reference. In Figure 3.9 we show the projected uncertainties of the azimuthal anisotropy v_2 compared with the

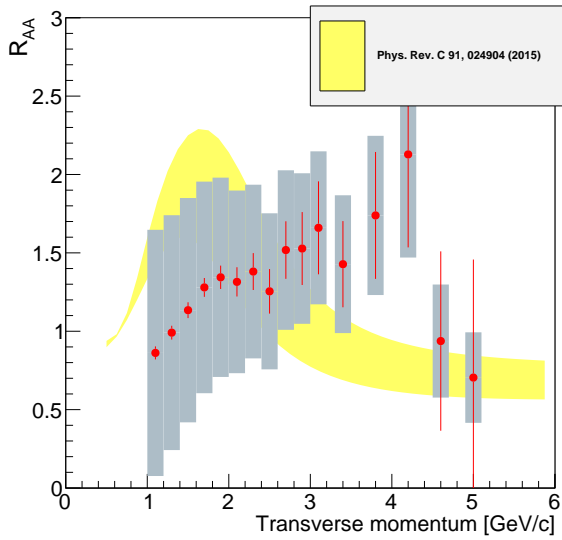


Figure 3.7: Comparison of measured heavy flavor electron R_{AA} uncertainties in minimum bias 62.4 GeV collisions compared to a model by Rapp *et al.*

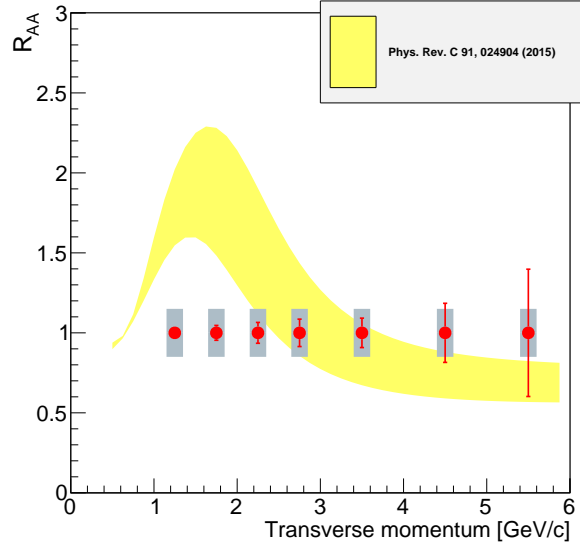


Figure 3.8: Comparison of projected heavy flavor electron R_{AA} uncertainties in minimum bias 62.4 GeV collisions compared to a model by Rapp *et al.*

same model. Together, measurements of the heavy flavor electron v_2 and R_{AA} at 62.4 GeV can help to determine whether the surprising modification of heavy flavor in the medium created at 200 GeV is due to the high energy density or by an increase in coupling strength near the transition temperature [22].

In addition to the measurement of heavy flavor electrons at mid-rapidity, muons from heavy flavor decays can be measured at forward rapidity with the FVTX detector. In Au+Au collisions such a measurement can provide further constraints on both medium interaction and initial state effects. Furthermore, the rapidity dependence of charm yields in $p+p$ can provide constraints on the charm production itself, which has large theoretical uncertainties. Figure 3.11 shows the projected uncertainties of R_{AA} from charm and bottom decays at forward rapidity.

Another exciting physics measurement is that of thermal photons in Au+Au at 62.4 GeV. The comparison of the thermal photon emission between such a new measurement at 62.4 GeV and our published results at 200 GeV would be very illuminating. Some theoretical explanations that attempt to reconcile the Au+Au 200 GeV thermal photon yield and flow coefficients require stronger coupling near the transition temperature — see for example Ref. [10] titled “Pseudo-Critical Enhancement of Thermal Photons in Relativistic Heavy-Ion Collisions”. These calculations predict larger such effects when the early stage quark-gluon plasma is closer to the transformation temperature. There are even more exotic calculations predicting a large v_2 due to magnetic fields in the medium.

To sort out the so-called “direct photon puzzle”, variation in the collision energy and geometry will be required. The method that can be employed to measure direct photons at low momentum is via external conversions that are tagged by their location in the barrel silicon vertex detector, which

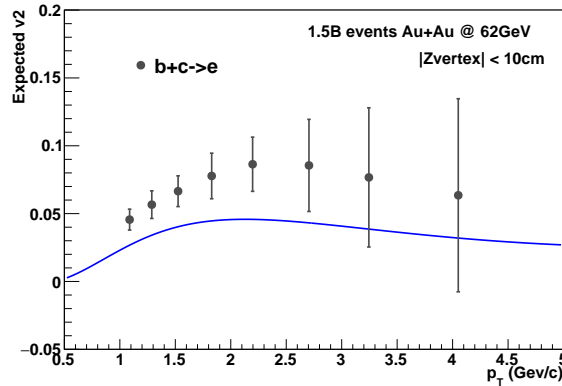


Figure 3.9: Comparison of measured heavy flavor electron v_2 uncertainties in minimum bias 62.4 GeV collisions compared to a model by Rapp *et al.*

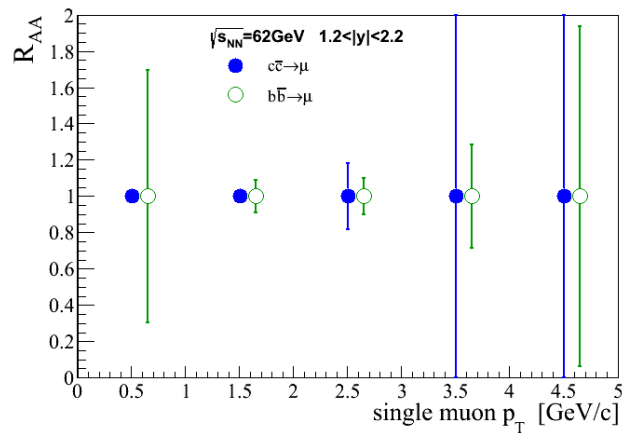


Figure 3.10: Projected uncertainties of heavy flavor muon R_{AA} for central 0-20% Au+Au 62.4 GeV collisions.

is same method used in the PHENIX publication for 200 GeV from conversions in the back-plane of the HBD [23]. The overall combinatorial background is lower for Au+Au at 62.4 GeV and the pointing to the conversion location in the VTX is good. Although ongoing analysis of the 62.4 GeV data from Run-10 may provide a precise measurement of the effective temperature, more statistics will be required for a measurement of v_2 . Figure 3.11 shows the projected uncertainties for direct photon v_2 from 5 weeks of Au+Au running.

3.3.1 Spin physics at 62.4 GeV

As mentioned above, there may be a trade-off between total $p+p$ running time and integrated luminosity and the desire for polarization of the protons during this running period. If running with longitudinal polarization, one can make a significant measure of the neutral pion A_{LL} in the PHENIX Central Arms, as shown in Figure 3.12.

C-AD projections indicate that the precision measurement potential of even two weeks of running

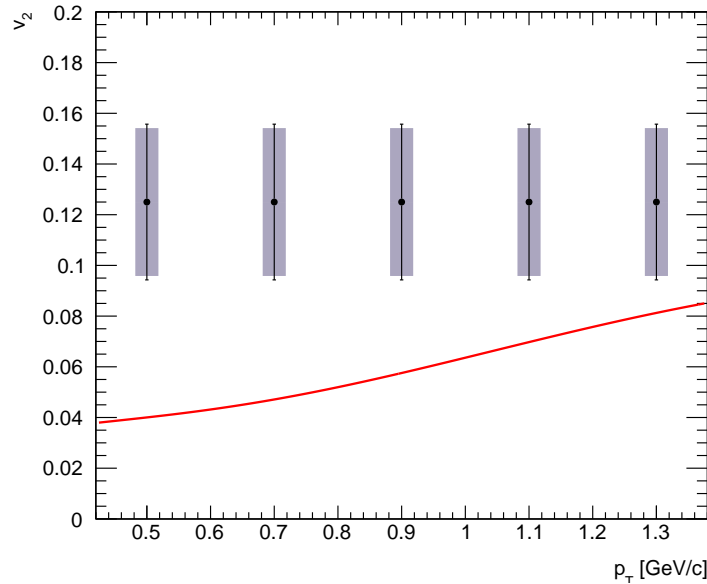


Figure 3.11: Projected uncertainties for direct photon v_2 in minimum bias 62.4 GeV Au+Au collisions. The curve is from [24].

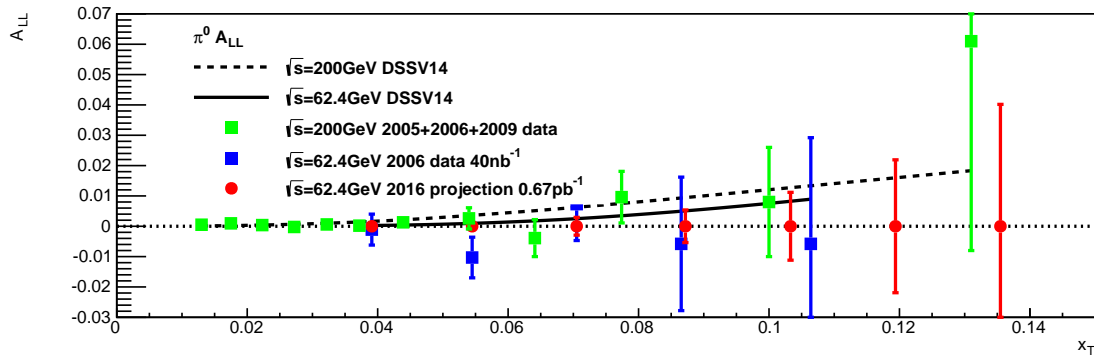


Figure 3.12: Projected uncertainties the neutral pion A_{LL} in comparison with previous measurements and different theoretical projections.

time at 62.4 GeV would allow one to see and confirm the nonzero asymmetries due to the nonzero gluon polarization [25] recently obtained, based predominantly on the 200 GeV RHIC data. In fact, the C-AD estimate of the fraction of events within $|z| < 30$ cm seems quite conservative, and we expect that one might sample a higher integrated luminosity for these measurements. The projected asymmetry measurement would extend to higher x than previous PHENIX results, indicated in Figure 3.12 as a function of $x_T = 2p_T/\sqrt{s}$, and would extend overlap with x values previously only covered by the STAR jet measurement [26]. The measurement would not have quite the precision of the STAR result, but it would serve as a very important cross check in this region.

A very intriguing exploratory measurement is to look for azimuthal asymmetries in forward neutral pion production in the MPC detectors with one beam polarized longitudinally and the

other polarized transversely [27]. C-AD has confirmed that the accelerator can be operated in this cross-polarized mode. Given the large single spin asymmetries observed in proton-proton collisions, such double spin asymmetries A_{LT} could be substantial as well. There are currently no theoretical calculations on the expected size of such an asymmetry, but the possible contributions have been laid out in Ref. [27]. If found to be nonzero, it could help improve the understanding of the mechanisms which also create the large single spin asymmetries and stimulate more theoretical progress on these asymmetries. In particular, fragmentation effects as well as quark-gluon-quark correlations in the proton are expected to contribute to A_{LT} in combination with the gluon helicity of the longitudinally polarized proton. As shown in Figure 3.13, the existence of such asymmetries can be tested at the 1% level for x_F where the single spin asymmetries reach 10% at the same center-of-mass energy [28]. Similar to the case of single spin asymmetries, here there is a transverse momentum dependent distribution function, g_{1T} , that is related via moments and has been found to be nonzero in semi-inclusive deep inelastic scattering [29, 30].

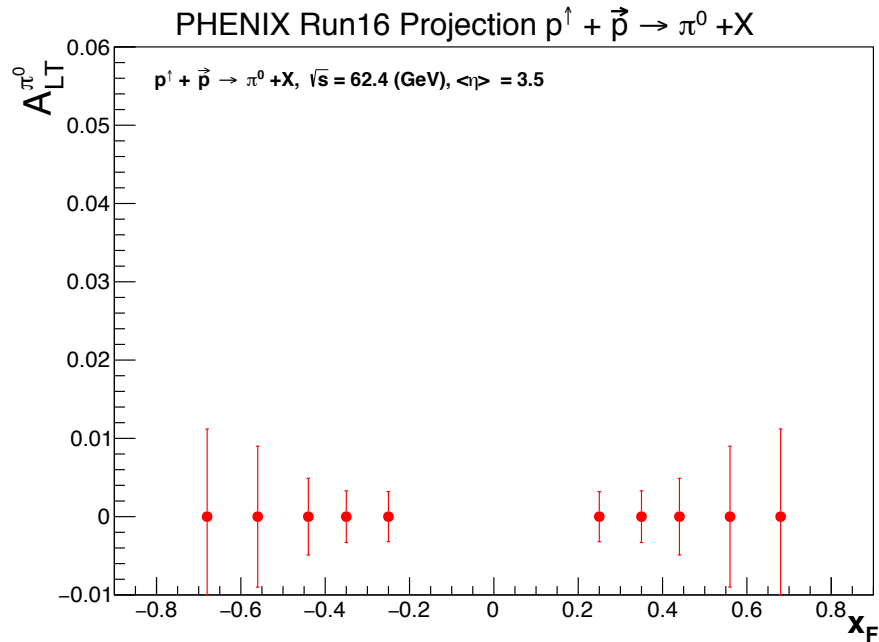


Figure 3.13: Expected double spin asymmetries A_{LT} uncertainties for neutral pions at $\langle \eta \rangle = 3.5$ for an accumulated luminosity of 0.67 pb^{-1} and assuming a vertex within $|z| < 30 \text{ cm}$.

We expect data from this combination of $p+p$ and Au+Au running at 62.4 GeV to be a unique RHIC contribution to constraining our understanding of the temperature dependence of quark-gluon plasma properties and to the rich spin structure of the proton.

3.4 Run-16 Small-System ($d+A$) Beam Energy Scan

The discovery of flow-like patterns in high multiplicity $p+p$ and $p+Pb$ collisions [5, 31, 32, 33, 34] at the LHC and $d+Au$ collisions at RHIC [3, 35] has challenged our understanding of perfect fluid hydrodynamics and the minimal conditions necessary for quark-gluon plasma formation. Publications by the PHENIX collaboration from $d+Au$ collisions at 200 GeV recorded in the 2008 running period include elliptic flow coefficients, their particle species dependence, as well as the centrality dependent HBT source sizes [3, 35, 36]. The STAR collaboration has confirmed the existence of a long-range near-side ridge correlation in $d+Au$, though with a different interpretation of the away-side enhanced yield [37, 38]. Already preliminary analysis of $^3\text{He}+Au$ collisions at 200 GeV recorded at the end of the 2014 running period indicate substantial elliptic and triangular flow coefficients as shown in Figure 1.1. Another puzzle in the field comes from nucleus-nucleus collisions at lower energies with data taken as part of the Beam Energy Scan - Phase 1, where the elliptic flow coefficients show only a modest collision energy dependence [39].

In order to test competing underlying physics explanations, we explore here options for a Beam Energy Scan of small system collisions ($d+Au$ and/or $^3\text{He}+Au$) collisions over the collision energy range 20–200 GeV. Initial calculations of the expected elliptic and triangular flow over this collision energy range from a model (superSONIC) with pre-equilibrium dynamics, viscous hydrodynamics, and finally hadronic cascade were published in Ref. [40]. Shown in Figure 3.14 are calculations for v_2 and v_3 as a function of transverse momentum in central $d+Au$ collisions from superSONIC. These results are all for a quark-gluon plasma as modeled by viscous hydrodynamics with $\eta/s = 1/4\pi$ and a transition temperature to hadronic cascade at $T = 170$ MeV. It is striking that the v_2 remains substantial at all collision energies, with a reduction of approximately 25% at all p_T from the highest to the lowest energy. This modest change is despite a significant change in the initial temperature and thus a shortening of the time spent in the viscous hydrodynamic, i.e. quark-gluon plasma, stage. In contrast, the v_3 has a dramatic drop in going from collisions at 62 to 39 GeV and a total reduction of 60% from the highest to the lowest energy. This follows a trend that the triangular flow takes more time to develop and a very short time in the quark-gluon plasma, low viscosity phase, does not allow the spatial anisotropy to translate to momentum space [4].

It has recently been shown that A-Multi-Phase-Transport (AMPT) [41] calculations are able to describe many features of the LHC $p+p$ and $p+Pb$ flow-like patterns [42], and this is also true for $d+Au$ and $^3\text{He}+Au$ features at RHIC [43]. The exact understanding of the underlying physics responsible for producing these features is not yet clear, though interesting studies [44] indicate a role for surface emission — a so-called “escape mechanism” — combined with later parton coalescence. We have run AMPT for central $d+Au$ collisions at 20, 39, 62, and 200 GeV and show the two-particle, rapidity-separated correlations in Figure 3.15. The striking feature is that the near-side ridge, as a distinct peak in the two-particle correlation is barely visible at 39 GeV and completely gone at 20 GeV collision energy.

RHIC is uniquely capable of carrying out this small-system Beam Energy Scan. It will provide crucial data to further constrain the physics of rapid equilibration and the applicability of viscous hydrodynamics to small systems. We considered three possible small-systems for this Beam Energy Scan: $p+Au$, $d+Au$, and $^3\text{He}+Au$. As documented in the C-AD “RHIC Collider Projections (FY2016-2022)” [45], both $p+Au$ and $^3\text{He}+Au$ are “only possible without the Coherent electron Cooling (CeC) undulator” which is planned to be in place in 2016. In contrast “with the CeC

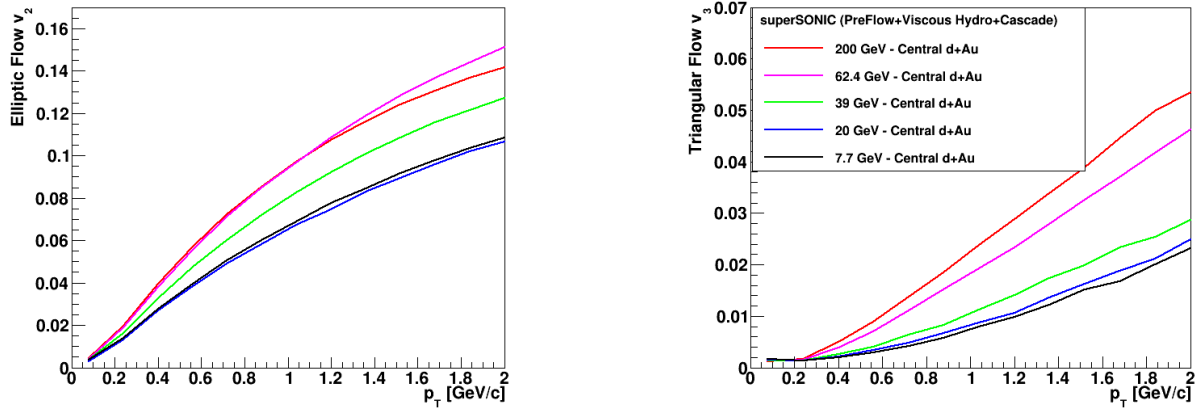


Figure 3.14: Shown are predictions for $d+Au$ collisions at collision energies = 7.7, 20, 39, 62, 200 GeV from the superSONIC hydrodynamic model for v_2 (left) and v_3 (right) as a function of transverse momentum.

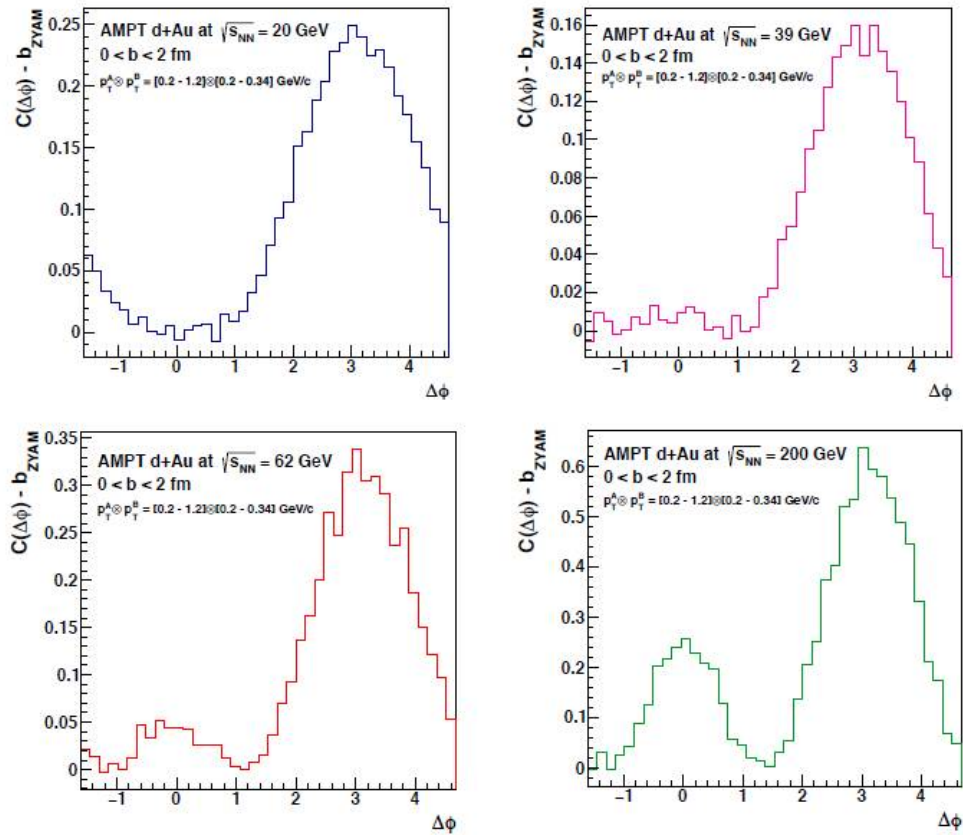


Figure 3.15: Shown are predictions two-particle, rapidity-separated correlations for $d+Au$ collisions at collision energies = 20, 39, 62, 200 GeV from the AMPT model.

beam energy [GeV/nucleon]	h+Au	d+Au	L in $ z <30$ cm [%]	L in $ z <10$ cm [%]	comment
	luminosity [nb ⁻¹ /week]	luminosity [nb ⁻¹ /week]			
100	33	110	50	20	Run-14 performance for h+Au
31.2	3.3	10.6	50	20	197 MHz on, cooling on for Au
19.5	1.2	3.8	50	20	197 MHz on, cooling off for Au
9.8	0.3	0.9	15	5	197 MHz off, cooling off for Au

Figure 3.16: Shown are projected luminosities for small-system collisions over a range of collision energies.

undulator $d+Au$ collisions at these energies are possible.” The CeC test is a critical component of Electron Ion Collider (EIC) R&D for the accelerator.

The above viscous hydrodynamic and AMPT calculations are shown for $d+Au$ collisions, and calculations for $^3\text{He}+Au$ show similar results, with expected higher v_3 values in $^3\text{He}+Au$. The projected luminosities for $d+Au$ are significantly higher than for $^3\text{He}+Au$, and so that appears to be the optimal solution. We note that a key aspect of the scan is to have the same detector configuration and capabilities at all energies. That requires a short $d+Au$ run at 200 GeV as the baseline, since the earlier 2008 $d+Au$ run did not include the forward silicon vertex detector (FVTX) covering pseudo-rapidity $\eta = 1.0 - 3.0$ that has provided excellent event-plane determination in the recent $^3\text{He}+Au$ run in 2014.

The projected luminosities in $d+Au$ (and $^3\text{He}+Au$ for completeness) are shown in Figure 3.16. For the FVTX to have optimal acceptance, the collisions should take place within $|z| < 10$ cm. With the high-speed PHENIX data acquisition, we can effectively record all 0-5% central collisions at all energies, in addition to a substantial minimum bias event sample. Factoring in the expected PHENIX experiment 70% uptime, we calculate the number of 0–5% central collisions that can be recorded. An example run plan utilizing input from C-AD is as follows:

- 0.5 week setup
- 1.5 week $d+Au$ 200 GeV
- 0.5 week change
- 1.5 week $d+Au$ 62 GeV
- 0.5 week change
- 2.0 week $d+Au$ 39 GeV
- 0.5 week change
- 2.0 week $d+Au$ 20 GeV

This plan will yield 2.4 billion, 230 million, 110 million, and 7 million central $d+Au$ events at energies of 200, 62, 39, 20 GeV respectively. Shown in Figure 3.17 are the projected flow coefficient uncertainties corresponding to the data samples achievable. These uncertainties are based on the statistical sample combined with the superSONIC projections, also shown. We are thus

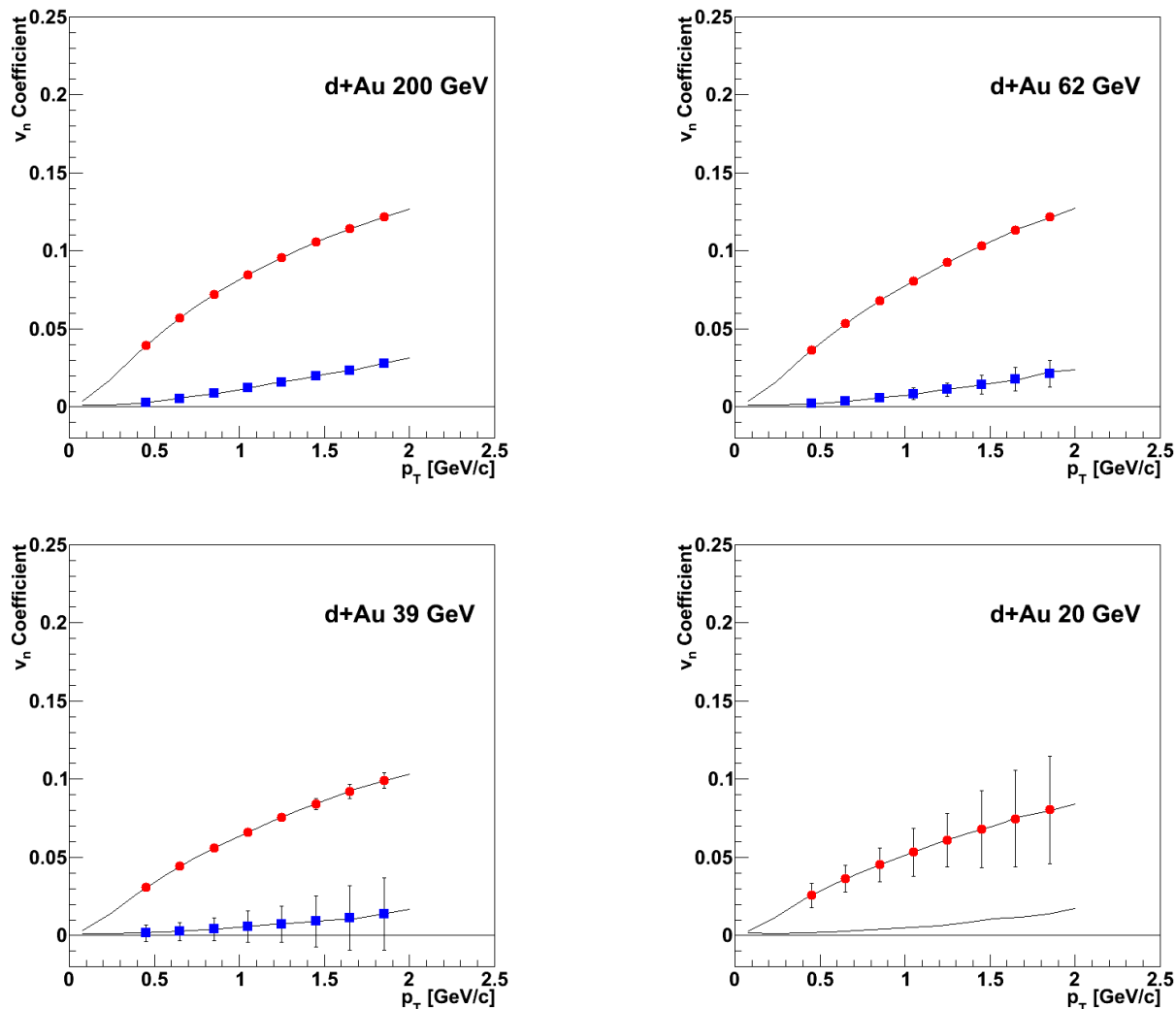


Figure 3.17: Shown are projected uncertainties for measurements of v_2 and v_3 coefficients in 0-5% central $d+Au$ collisions at 200, 62, 39, and 20 GeV energies in the top left, top right, lower left, and lower right panels respectively. For the much smaller data sample at the lowest energy of 20 GeV, we do not quote projected uncertainties for v_3 since it is not clear if the event-plane method determination will be robust.

confident that an excellent data sample can be obtained with important physics ramifications for the understanding of the minimal conditions for quark-gluon plasma formation, its evolution, and potential alternative explanations.

The Collaboration is excited to extend these small-system tests to the limit in both size and energy. In addition to the measurement of these flow coefficients, we find that other correlations and initial state effects measured at these energies will provide useful input to the Au+Au Beam Energy Scan program.

3.5 Options for $p+p$ at 510 GeV Running

The Collaboration has continued, strong interest in the polarized $p+p$ at 510 GeV program, both in longitudinal and transverse spin physics. However, we anticipate the potential for a modest length $p+p$ at 510 GeV run in Run-16 (incorporating set-up and ramp-up times) to be insufficient to warrant a proposal. Again, we note that the PHENIX detector will not be taking data in Run-17. Nonetheless, we briefly detail here some of the exciting measurements in both transverse and longitudinal spin running still to be made.

The physics with transverse polarization has a substantial continued interest related to the Sivers distribution function, via the azimuthal single-spin asymmetry of Drell-Yan (DY) lepton pairs. The current understanding of how gauge links between interacting quarks and proton remnants cause these asymmetries to exist predicts a sign-change when extracting the Sivers function from DY in comparison to existing semi-inclusive DIS measurements. This measurement is planned to be realized in STAR via full W reconstruction, in COMPASS via π^- beams on proton target induced DY muon pairs, and potentially at RHIC via Drell-Yan pairs with upgraded forward sPHENIX upgrades – as detailed in the White Paper submitted last year [46], as well as comparable STAR forward upgrades.

The capabilities with the current PHENIX detector system have been evaluated using the Run-13 $p+p$ at 510 GeV data. Initial findings show that di-muons in the mass range 4–9 GeV in the PHENIX muon arms ($1.4 < |\eta| < 2.4$) can reach a signal to background of unity at the cost of acceptance/efficiency. If one were to have additional running as long as Run-13 but with twice the luminosity delivered, it would correspond to uncertainties on the order of 10% which would barely reach the maximum of the most optimistic predictions of these asymmetries. Several efforts are underway for PHENIX and fsPHENIX together to significantly improve the background rejection in order to make this measurement feasible. Apart from various selection optimizations, hardware changes for PHENIX have also been considered, and they will be discussed below. There is also a feasibility study as to whether a measurement of low-mass DY muon pairs is a possibility with the existing PHENIX detector. Low-mass muon DY muon pairs are more abundant and initial studies indicate that the background can be removed very effectively via high momentum and other selection criteria. The problem with such a potential measurement is that these cuts would force the measurements into a range where the transverse momentum of the DY pair is of the same order or even larger than the invariant mass, which means the TMD formalism to describe these asymmetries in terms of the Sivers function is no longer applicable and the theoretical interpretation of such results would be difficult.

In addition, in $p+p$ at 510 GeV, direct photon transverse spin asymmetry measurements are possible but become more difficult compared to the situation at 200 GeV. At forward rapidities the energies of neutral pions and direct photons increase which will limit their distinction even with the new MPC-EX detector to photon energies of below 80 GeV. As substantial pion asymmetries have only been seen for $x_F > 0.3$, the overlap would be limited.

In terms of longitudinal polarization, additional running of $p+p$ at 510 GeV would improve the measurements related to the ΔG and W programs. With the 510 GeV data taken in Run-13 both the central neutral pion and the forward cluster double spin asymmetries are expected to reach statistical precision better than the systematic uncertainties at small transverse momenta. Recently, the understanding of the dominant systematic uncertainties from the relative luminosity

measurements has significantly improved, likely resulting in substantially smaller uncertainties. Since these regions are the most relevant for extending the knowledge of the gluon polarization toward smaller x the expected impact can be improved still with additional statistics. In addition, also here, the recently installed MPC-EX detector should improve the detection of pions toward higher transverse momenta than possible with the detector setup existing in Run-13 and thus improve the purity of the measurement from clusters to pions. Also the slightly larger than expected preliminary results for the Run-13 central neutral pions at intermediate to larger transverse momenta would make additional statistics in these regions very interesting.

For the $W \rightarrow \mu$ at forward rapidity program additional statistics alone will not benefit the measurement substantially, as currently the uncertainties on the preliminary Run-13 results at forward rapidities are dominated by the uncertainties on the signal-to-background extraction. Since the signal-to-background is still relatively low at around 1/2 increasing this ratio is the main goal in improving the forward W measurements. Apart from modest improvements still being expected between the preliminary and final results other modest improvements could be expected by having the full set of vertex detectors installed in comparison to Run-13 where only the FVTX was fully operational due to the cooling leaks in the VTX. It has been shown, that the FVTX detector can catch jet-like activity around the candidate W decay muon and thus reject various backgrounds. However, only about 30% of the events pass through enough layers of the FVTX so the additional information from the VTX would be beneficial to a large fraction of events and additionally also away-side jets might be vetoed. In addition to this software effort to improve the significance and potential impact of additional data on the W program also two hardware suggestions are being considered despite being for (or rather after) the very last run PHENIX is going to participate in before the preparations for sPHENIX.

One is a rather straightforward addition of two more interaction lengths of absorber such as stainless steel around the central interaction region. This would mostly eliminate any remaining hadron background among the muon candidates (predominantly low momentum hadrons punching through all absorbing material and decaying within the muon tracker volume). With such an additional absorber a signal to background of unity should be achieved. Unfortunately, such an absorber would prohibit any central arm measurements while keeping the MPC double spin capabilities. The other, more sophisticated option would be to replace the current Cu nosecones and instrument them with scintillators, sandwiched between absorbing material. This would allow one to measure the energy of particles and jets and thus allow to veto them better than via multiplicity criteria as performed by the FVTX. Several parts of this technology, especially the readout, are being tested already for future sPHENIX and EIC detectors.

As mentioned in Section 1.1, CMS observes a near-side ridge in $p+p$ events selected using a high multiplicity track trigger [5]. The CMS trigger condition, >110 charged tracks in their acceptance, corresponds to an average multiplicity of about ~ 28 per unit rapidity. Motivated by the potential for pursuing this physics measurement at RHIC, PHENIX has developed an FVTX high multiplicity trigger. Its performance in $p+p$ and $p+Au$ at 200 GeV in Run15 is discussed in Section 2.1. This trigger could also enhance the sample of high multiplicity events at 510 GeV, in which one sees a higher multiplicity and a stronger correlation in the multiplicity over a wide rapidity gap. Figure 3.18 shows the track multiplicities measured in the FVTX for 200 GeV and 510 GeV. The 510 GeV distribution has a tail towards higher multiplicity which provides a statistical advantage for these high multiplicity events. Figure 3.18 also shows the correlation of the track multiplicity in FVTX North and South acceptances for $p+p$ at 200 GeV and 510 GeV.

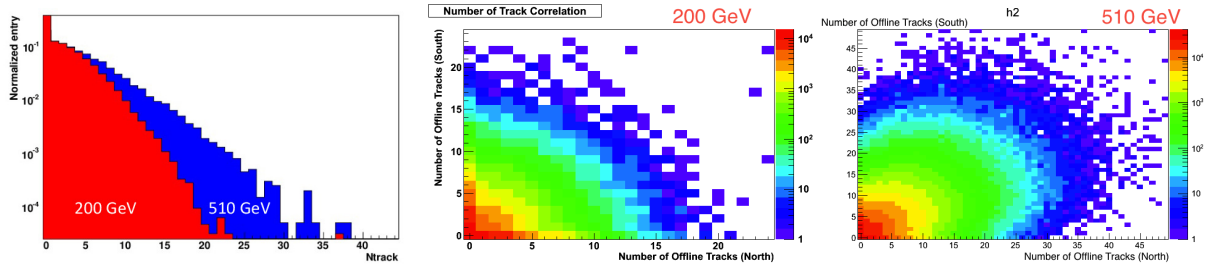


Figure 3.18: (left) The track multiplicity distributions in FVTX per arm for $p+p$ collisions at 200 GeV and 510 GeV based on data from Run15 and Run13, respectively. Track multiplicity correlation between North and South FVTX for 200 GeV (middle) and 510 GeV (right).

Again, these are physics areas in transversely and longitudinally polarized $p+p$ at 510 GeV, or in high multiplicity triggered $p+p$ events at 510 GeV, where detector improvements and additional running would have impactful physics results. However, given the constraints on running time and PHENIX data taking only in Run-16, we cannot place these as high priority.

Chapter 4

sPHENIX

The PHENIX Collaboration has a proposal to replace PHENIX with a new detector, sPHENIX, aimed at investigating the physics underpinning the emergent phenomena of the quark-gluon plasma. The sPHENIX detector is designed with outstanding capabilities for fully calorimetric measurements of jets, heavy-flavor tagged jets, direct photons, upsilons, high p_T Ds, and high p_T charged hadrons. The updated proposal was submitted to the DOE in November 2014 and completed an extremely positive DOE review of its science case in April 2015.

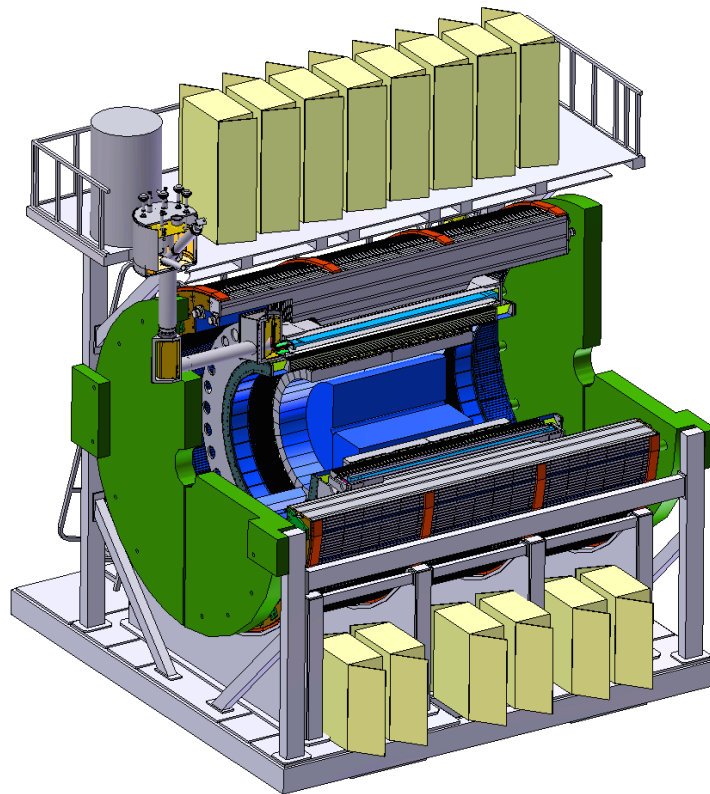


Figure 4.1: Engineering rendering of sPHENIX with its support structure.

Figure 4.1 shows an engineering drawing of the sPHENIX detector with the support structure, cryogenic chimney, and platforms for electronic racks. In radial order, the drawing shows the tracking and vertexing system, the electromagnetic calorimeter, the inner segment of the hadronic calorimeter, the BaBar 1.5 T superconducting solenoid, and the outer segment of the hadronic calorimeter. The magnetic flux is contained and shaped by the green end cap doors.

The tracking system is capable of $\sigma_{\text{DCA}} < 100 \mu\text{m}$, enabling b -tagging of jets, and has a mass resolution of better than $100 \text{ MeV}/c^2$, enabling the separate identification of the $Y(1S)$, $Y(2S)$, and $Y(3S)$ states. The calorimeters enable very low-bias triggering of jets in $p+p$ and $p+\text{Au}$. The tracking and calorimetry together enable a variety of modern jet reconstruction approaches to be employed in $p+p$, $p+\text{Au}$ and $\text{Au}+\text{Au}$. The DAQ reads out at 15 kHz, which is well matched to C-AD's $\text{Au}+\text{Au}$ luminosity projections, and enables sPHENIX to collect outright a minimum bias sample of 100 billion $\text{Au}+\text{Au}$ events and to sample 0.6 trillion events with the calorimeters. This latter capability to fully exploit the excellent RHIC luminosity is particularly important for targeted observables such as photon-jet correlations.

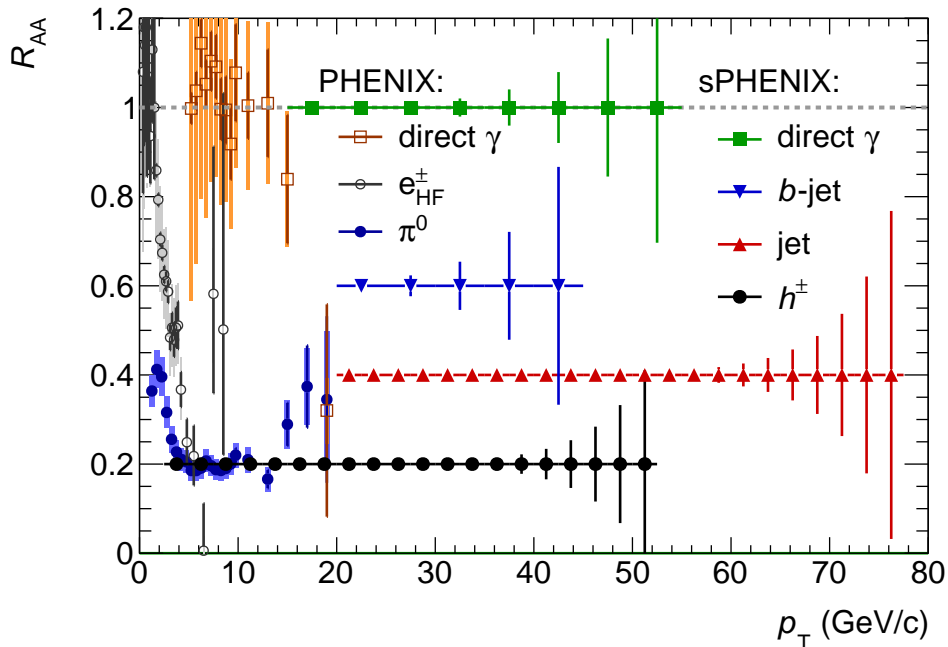


Figure 4.2: Statistical projections for the R_{AA} of various hard probes vs p_T in 0–20% Au+Au events with the sPHENIX detector after two years of data-taking, compared with a selection of current hard probes data from PHENIX.

The full physics case for sPHENIX is described in detail in the proposal [47]. In conjunction with existing and anticipated measurements at the LHC, the new capabilities for hard probes and beauty quarkonia at RHIC probe the strongly coupled QGP in the vicinity of T_c , providing access to physics over an important range of temperatures, length scales, and virtualities. One way to see the impact sPHENIX will have is shown in Figure 4.2 by the greatly extended kinematic reach of the direct photons, light and heavy flavor jets and charged hadrons of sPHENIX over the comparable hard

sPHENIX

process observables of PHENIX.



Figure 4.3: The BaBar solenoid, shipped from SLAC in January 2015, is now in Bldg. 912 undergoing testing.

There have been other recent sPHENIX developments. Very notably, the BaBar superconducting solenoid, which forms the centerpiece of the experiment, was successfully shipped by truck from SLAC to BNL in February 2015. Figure 4.3 shows the solenoid soon after it was rigged into a temporary location in AGS Bldg. 912, where it is currently undergoing a battery of acceptance tests. The Collaboration is energized about the sPHENIX physics program and eager to realize it as an detector.

Appendix A

Beam use proposal charge

Date: April 24, 2015 Final version of the Beam Use Request, for the records:

Dear RHIC Spokespersons:

In consultation with the Office of Nuclear Physics we have decided to make a change to the future RHIC run schedule. Specifically, we now plan to run RHIC in both FY16 and FY17, followed by one year (FY18) without a RHIC run during which the low energy RHIC electron cooling (LEReC) system will be installed. The high statistics Beam Energy Scan II is then planned for the years FY19 and FY20. The modified plan will allow for a less aggressive schedule of the LEReC project. It will also relax the conflict between the heavy ion and spin physics programs of RHIC that remained unresolved at last year's PAC meeting.

I request that you submit the annual beam use requests by May 19, 2015. The BURs should be for a 22-week RHIC run in FY16, and either a 15-week or a 22-week RHIC run in FY17.

I also ask the STAR Collaboration to present the iTPC proposal to the PAC and to provide an update on experimental efforts aimed at exploring possible phenomenological manifestations of the chiral magnetic effect.

Both collaborations should present a tentative schedule for the release of results from the data taken in runs 13 and 14 (p+p, Au+Au 15 GeV, Au+Au 200 GeV, 3He+Au).

Thanks, Berndt

Bibliography

- [1] PHENIX Collaboration. Phenix collaboration beam use proposal for run-15 and run-16 (submitted in 2014) [online]. URL: <http://www.phenix.bnl.gov/phenix/WWW/publish/dave/PHENIX/BUP14.pdf>. (document)
- [2] A. Adare et al. Heavy-quark production and elliptic flow in Au+Au collisions at $\sqrt{s_{NN}} = 62.4$ GeV. 2014. arXiv:1405.3301. (document), 3.3
- [3] A. Adare et al. Measurement of long-range angular correlation and quadrupole anisotropy of pions and (anti)protons in central d +Au collisions at $\sqrt{s_{NN}}=200$ GeV. 2014. arXiv:1404.7461. 1.1, 3.4
- [4] J.L. Nagle, A. Adare, S. Beckman, T. Koblesky, J. Orjuela Koop, et al. Exploiting Intrinsic Triangular Geometry in Relativistic He3+Au Collisions to Disentangle Medium Properties. *Phys.Rev.Lett.*, 113(11):112301, 2014. arXiv:1312.4565, doi:10.1103/PhysRevLett.113.112301. 1.1, 3.4
- [5] Vardan Khachatryan et al. Observation of Long-Range Near-Side Angular Correlations in Proton-Proton Collisions at the LHC. *JHEP*, 1009:091, 2010. arXiv:1009.4122, doi:10.1007/JHEP09(2010)091. 1.1, 3.4, 3.5
- [6] A. Adare et al. Beam-energy and system-size dependence of the space-time extent of the pion emission source produced in heavy ion collisions. 2014. arXiv:1410.2559. 1.2
- [7] S. S. Adler et al. Transverse-energy distributions at midrapidity in $p + p$, $d + Au$, and $Au + Au$ collisions at $\sqrt{s_{NN}} = 62.4 \sim 200$ gev and implications for particle-production models. *Phys. Rev. C*, 89:044905, Apr 2014. URL: <http://link.aps.org/doi/10.1103/PhysRevC.89.044905>, doi:10.1103/PhysRevC.89.044905. 1.2
- [8] A. Adare et al. Systematic study of charged-pion and kaon femtoscopy in Au+Au collisions at $\sqrt{s_{NN}}=200$ GeV. 2015. arXiv:1504.05168. 1.3
- [9] A. Adare et al. Observation of direct-photon collective flow in $\sqrt{s_{NN}} = 200$ GeV Au+Au collisions. 2011. arXiv:1105.4126. 1.3
- [10] Hendrik van Hees, Min He, and Ralf Rapp. Pseudo-Critical Enhancement of Thermal Photons in Relativistic Heavy-Ion Collisions. *Nucl.Phys.*, A933:256–271, 2015. arXiv:1404.2846, doi:10.1016/j.nuclphysa.2014.09.009. 1.3, 3.3
- [11] A. Adare et al. Measurement of parity-violating spin asymmetries in W^\pm production at midrapidity in longitudinally polarized $p+p$ collisions. 2015. arXiv:1504.07451. 1.4

- [12] Ralf Seidl. PHENIX W to μ measurements in polarized proton-proton collisions. *PoS, DIS2014:205*, 2014. 1.4
- [13] P. Lees, J. et al. Search for a dark photon in e^+e^- collisions at *BaBar*. *Phys. Rev. Lett.*, 113:201801, Nov 2014. URL: <http://link.aps.org/doi/10.1103/PhysRevLett.113.201801>, doi:10.1103/PhysRevLett.113.201801. 1.5
- [14] Evgueni Goudzovski. Search for the dark photon in π^0 decays by the NA48/2 experiment at CERN. 2014. arXiv:1412.8053. 1.5
- [15] C. Aidala et al. The PHENIX Forward Silicon Vertex Detector. *Nuclear Instruments and Methods in Physics Research A*, accepted for publication, 2014. arXiv:physics.ins-det/1311.3594v2. 2.1
- [16] A. Adare et al. Nuclear modification of ψ' , χ_c and J/ψ production in d+Au collisions at $\sqrt{s_{NN}} = 200$ GeV. *Phys.Rev.Lett.*, 111:202301, 2013. arXiv:1305.5516, doi:10.1103/PhysRevLett.111.202301. 2.1
- [17] B. Abelev et al. J/ψ Production as a Function of Charged Particle Multiplicity in pp Collisions at $\sqrt{s} = 7$ TeV. *Phys.Lett.*, B712:165–175, 2012. arXiv:1202.2816, doi:10.1016/j.physletb.2012.04.052. 2.1
- [18] V. Blobel. Software alignment for tracking detectors. *Nucl.Instrum.Meth.*, A566:5–13, 2006. doi:10.1016/j.nima.2006.05.157. 2.2
- [19] C-AD Run-14 and Run-15 Projection Document (provided by W. Fischer). URL: <http://www.rhichome.bnl.gov/RHIC/Runs/RhicProjections.pdf>. 3.1
- [20] NPP Program Advisory Committee. Npp program advisory recommendation report 2014 [online]. URL: <http://www.bnl.gov/npp/docs/pac0614/Overallrecommendationsfinal.pdf>. 3.2
- [21] Talk at the 30th Winter Workshop on Nuclear Dynamics, Barbara Trzeciak for the STAR Collaboration. URL: <http://indico.cern.ch/event/275088/contribution/71/material/slides/0.pdf>. 3.3
- [22] Min He, Rainer J. Fries, and Ralf Rapp. Modifications of heavy-flavor spectra in $\sqrt{s_{NN}} = 62.4$ gev au-au collisions. *Phys. Rev. C*, 91:024904, Feb 2015. URL: <http://link.aps.org/doi/10.1103/PhysRevC.91.024904>, doi:10.1103/PhysRevC.91.024904. 3.3
- [23] A. Adare et al. Centrality dependence of low-momentum direct-photon production in Au+Au collisions at $\sqrt{s_{NN}} = 200$ GeV. 2014. arXiv:1405.3940. 3.3
- [24] O. Linnyk, W. Cassing, and E. L. Bratkovskaya. Centrality dependence of the direct photon yield and elliptic flow in heavy-ion collisions at $\sqrt{s_{NN}} = 200$ gev. *Phys. Rev. C*, 89:034908, Mar 2014. URL: <http://link.aps.org/doi/10.1103/PhysRevC.89.034908>, doi:10.1103/PhysRevC.89.034908. 3.11
- [25] Daniel de Florian, Rodolfo Sassot, Marco Stratmann, and Werner Vogelsang. Evidence for polarization of gluons in the proton. 2014. arXiv:1404.4293. 3.3.1

- [26] L. Adamczyk et al. Precision Measurement of the Longitudinal Double-spin Asymmetry for Inclusive Jet Production in Polarized Proton Collisions at $\sqrt{s} = 200$ GeV. 2014. arXiv:1405.5134. 3.3.1
- [27] A. Metz, D. Pitonyak, A. Schaefer, and J. Zhou. Analysis of the double-spin asymmetry A_{LT} in inelastic nucleon-nucleon collisions. *Phys.Rev.*, D86:114020, 2012. arXiv:1210.6555, doi:10.1103/PhysRevD.86.114020. 3.3.1
- [28] A. Adare et al. Measurement of transverse-single-spin asymmetries for midrapidity and forward-rapidity production of hadrons in polarized p+p collisions at $\sqrt{s} = 200$ and 62.4 GeV. 2013. arXiv:1312.1995. 3.3.1
- [29] L.L. Pappalardo and M. Diefenthaler. Measurements of Double-Spin Asymmetries in SIDIS of Longitudinally Polarized Leptons off Transversely Polarized Protons. 2011. arXiv:1107.4227. 3.3.1
- [30] J. Huang et al. Beam-Target Double Spin Asymmetry A_{LT} in Charged Pion Production from Deep Inelastic Scattering on a Transversely Polarized ^3He Target at $1.4 < Q^2 < 2.7$ GeV². *Phys.Rev.Lett.*, 108:052001, 2012. arXiv:1108.0489, doi:10.1103/PhysRevLett.108.052001. 3.3.1
- [31] Serguei Chatrchyan et al. Multiplicity and transverse momentum dependence of two- and four-particle correlations in pPb and PbPb collisions. *Phys.Lett.*, B724:213–240, 2013. arXiv:1305.0609, doi:10.1016/j.physletb.2013.06.028. 3.4
- [32] Betty Bezverkhny Abelev et al. Long-range angular correlations of β , K and p in p-Pb collisions at $\sqrt{s_{NN}} = 5.02$ TeV. *Phys.Lett.*, B726:164–177, 2013. arXiv:1307.3237, doi:10.1016/j.physletb.2013.08.024. 3.4
- [33] Betty Abelev et al. Long-range angular correlations on the near and away side in p-Pb collisions at $\sqrt{s_{NN}} = 5.02$ TeV. *Phys.Lett.*, B719:29–41, 2013. arXiv:1212.2001, doi:10.1016/j.physletb.2013.01.012. 3.4
- [34] Georges Aad et al. Measurement of long-range pseudorapidity correlations and azimuthal harmonics in $\sqrt{s_{NN}} = 5.02$ TeV proton-lead collisions with the ATLAS detector. *Phys.Rev.*, C90(4):044906, 2014. arXiv:1409.1792, doi:10.1103/PhysRevC.90.044906. 3.4
- [35] A. Adare et al. Quadrupole anisotropy in dihadron azimuthal correlations in central d+Au collisions at $\sqrt{s_{NN}} = 200$ GeV. *Phys.Rev.Lett.*, 2013. arXiv:1303.1794. 3.4
- [36] N.N. Ajitanand et al. Comparison of the space-time extent of the emission source in d+Au and Au+Au collisions at $\sqrt{s_{NN}} = 200$ GeV. *Nucl.Phys.*, A931:1082–1087, 2014. arXiv:1404.5291, doi:10.1016/j.nuclphysa.2014.08.054. 3.4
- [37] L. Adamczyk et al. Long-range pseudorapidity dihadron correlations in d+Au collisions at $\sqrt{s_{NN}} = 200$ GeV. 2015. arXiv:1502.07652. 3.4
- [38] L. Adamczyk et al. Effect of event selection on jetlike correlation measurement in d+Au collisions at $\sqrt{s_{NN}} = 200$ GeV. *Phys.Lett.*, B743:333–339, 2015. arXiv:1412.8437, doi:10.1016/j.physletb.2015.02.068. 3.4

- [39] L. Adamczyk et al. Elliptic flow of identified hadrons in Au+Au collisions at $\sqrt{s_{NN}} = 7.7-62.4$ GeV. *Phys.Rev.*, C88:014902, 2013. arXiv:1301.2348, doi:10.1103/PhysRevC.88.014902. 3.4
- [40] M. Habich, J.L. Nagle, and P. Romatschke. Particle spectra and HBT radii for simulated central nuclear collisions of C + C, Al + Al, Cu + Cu, Au + Au, and Pb + Pb from $\sqrt{s} = 62.4 - 2760$ GeV. *Eur.Phys.J.*, C75(1):15, 2015. arXiv:1409.0040, doi:10.1140/epjc/s10052-014-3206-7. 3.4
- [41] Zi-Wei Lin, Che Ming Ko, Bao-An Li, Bin Zhang, and Subrata Pal. A Multi-phase transport model for relativistic heavy ion collisions. *Phys.Rev.*, C72:064901, 2005. arXiv:nucl-th/0411110, doi:10.1103/PhysRevC.72.064901. 3.4
- [42] Adam Bzdak and Guo-Liang Ma. Elliptic and triangular flow in p +Pb and peripheral Pb+Pb collisions from parton scatterings. *Phys.Rev.Lett.*, 113(25):252301, 2014. arXiv:1406.2804, doi:10.1103/PhysRevLett.113.252301. 3.4
- [43] J. D. Orjuela Koop, A. Adare, D. McGlinchey, and J.L. Nagle. Long-Range Azimuthal Correlations from Parton Scattering in Central p +Au, d +Au, and ^3He +Au Collisions at $\sqrt{s_{NN}} = 200$ GeV. 2015. arXiv:1501.06880. 3.4
- [44] Liang He, Terrence Edmonds, Zi-Wei Lin, Feng Liu, Denes Molnar, et al. Anisotropic parton escape is the dominant source of azimuthal anisotropy from A Multi-Phase Transport. 2015. arXiv:1502.05572. 3.4
- [45] RHIC Beam Projections [online]. URL: <http://www.rhichome.bnl.gov/RHIC/Runs/RhicProjections.pdf>. 3.4
- [46] PHENIX Collaboration. Future opportunities in p + p and p + a collisions at rhic with the forward sphenix detector [online]. URL: http://www.phenix.bnl.gov/phenix/WWW/publish/dave/sPHENIX/pp_pA_whitepaper.pdf. 3.5
- [47] A. Adare et al. The sPHENIX Upgrade Proposal [online]. 2014. URL: http://www.phenix.bnl.gov/phenix/WWW/publish/documents/sPHENIX_proposal_19112014.pdf. 4